



**Politecnico
di Torino**

POLITECNICO DI TORINO

Corso di Laurea Magistrale in Ingegneria Energetica e Nucleare
A.a. 2020/2021

Tesi di Laurea Magistrale

ITER-International Thermonuclear Experimental Reactor: joining technologies for ITER components

Relatori:

Prof. Monica Ferraris
Prof. Valentina Casalegno

Candidata:

Federica Maria Di Carlo

Ottobre 2021

ITER-International Thermonuclear Experimental Reactor:
joining technologies for ITER components.

Federica Maria Di Carlo

October 2021

CONTENTS

ABSTRACT	7
INTRODUCTION	9
CHAPTER 1	11
JOINING TECHNOLOGIES	11
1.1 ITER technologies	11
1.2 PFCs materials and configurations	15
1.3 Joining requirements	18
1.4 Joining for ITER	19
CHAPTER 2	22
TUNGSTEN-STEEL JOINTS	22
2.1 Diffusion bonding	22
2.2 Diffusion bonding by HIP	23
2.3 Functionally Graded Materials	32
2.4 Brazed joints	35
2.4.1 Brazing with powders	35
2.4.2 Brazing with liquid-forming interlayers and electroplating	36
2.4.3 Brazing with interlayers and foils	38
CHAPTER 3	49
EXPERIMENTAL STUDY	49
3.1 Introduction	49
3.2 Materials and methods	49
3.3 Brazed joints	50

3.3.1	Experimental technique	50
3.3.2	Results and microstructural analysis	52
3.3.2.1	W/Gemco [®] /steel joints	52
3.3.2.2	W/Cu/steel joints	59
3.4	Surface modification of steel	64
3.4.1	Experimental activity	65
	CONCLUSIONS	70
	BIBLIOGRAPHY	72

LIST OF FIGURES AND TABLES

<i>Figure 1: ITER structure [3]</i>	11
<i>Figure 2: Divertor structure [10]</i>	14
<i>Figure 3: PFCs material combination</i>	16
<i>Figure 4: Dome hypervapotron design [11]</i>	17
<i>Figure 5: SEM images of W/Ti and Ti/FMS interfaces [26]</i>	23
<i>Figure 6: Fracture surfaces of W/Ti/steel joints with a) Ti-100 μm, b) Ti-300 μm [27] as joining interlayer</i>	24
<i>Figure 7: SEM representations of the joint a-b) after HIP, c-d) after vacuum annealing with no D₂, and e-f) after deuterium exposure with a partial pressure of 1000 Pa [30]</i>	25
<i>Figure 8: SEM image of the W/Zr/steel joint [31]</i>	26
<i>Figure 9: SEM images of W/Zr and Zr/steel interfaces [31]</i>	26
<i>Figure 10: Example of plastic fracture of SS316L surface [32] after 2 h of HIP and tensile test</i>	27
<i>Figure 11: Microstructures of the W/steel joint without interlayer: a) sandblasted, and b) polished [33]</i>	28
<i>Figure 12: Microstructures of the W/steel joint with Ni interlayer: a) sandblasted-30 μm, b) polished-30 μm, c) sandblasted 50 μm, d) polished-50 μm [33]</i>	29
<i>Figure 13: SEM magnifications of the joint with the first HIP (700°C) [34]</i>	30
<i>Figure 14: fracture surface at the steel/Cu side of the joint (980°C) with the presence of Si-oxide [34]</i>	30
<i>Figure 15: Shear strength of the joints trends according to the type of HIP [34]</i>	31
<i>Figure 16: Example of a FGM Fe/W composites [37]</i>	32
<i>Figure 17: Cross-sections of uniform coatings and steel/W FGMs at different W vol. fractions: a) 0 %, b) 25 %, c) 50 %, d) 75%, e) 100%, f) FGM [36].</i>	33
<i>Figure 18: Trend of the FGMs thickness and width in relation to the plastic deformation [38]</i>	34
<i>Figure 19: Overview of tungsten and EUROFER interfaces [40]</i>	35
<i>Figure 20: W/Ni and Ni/steel SEM magnifications [45]</i>	37
<i>Figure 21: Brittle fracture at a) tungsten side, b) steel side [49]</i>	39
<i>Figure 22: SEM images of the two fracture modes [50]</i>	40
<i>Figure 23: V/Cu-50Ti/W seam with magnification of the compounds and filler zone with defects [51]</i>	40
<i>Figure 24: Cu-12Ge and Cu-25Ge after thermocycle process [52]</i>	41

<i>Figure 25: Compressive radial stresses and tensile radial stresses with a vanadium interlayer [53]</i>	42
<i>Figure 26: Tubular furnace (Carbolite) of the laboratory at DISAT-Politecnico di Torino</i>	51
<i>Figure 27: Structures of the performed joints</i>	52
<i>Figure 28: Macrography of sample a of W/Gemco/steel without applying additional pressure during brazing (980 °C) and without coating on steel surface</i>	53
<i>Figure 29: Image of sample b of W/Gemco®/steel joint with additional pressure (weight of W) during brazing (980°C) and sputtering of 400 nm.</i>	53
<i>Figure 30: FESEM image of the sample a at high magnification</i>	54
<i>Figure 31: FESEM image of the sample b at high magnification</i>	54
<i>Figure 32: FESEM images of c) steel surface with 400 nm of Cr sputtered, d) steel surface with 500 nm of Cr sputtered, e) steel surface with 700 nm of Cr sputtered</i>	55
<i>Figure 33: Elemental maps at the steel/Gemco® interface (sample b)</i>	57
<i>Figure 34: Elemental maps of the W/Gemco®/steel interface (sample b)</i>	58
<i>Figure 35: Image of the W/Cu/steel joint (1130°C) with 700 nm sputtering</i>	59
<i>Figure 36: FESEM image of the whole W/Cu/steel joint (sputtered 700 nm)</i>	60
<i>Figure 37: Steel/Cu interface of the W/Cu/steel joint (sputtered 700 nm)</i>	61
<i>Figure 38: EDS spectrum at Cu/steel interface</i>	62
<i>Figure 39: elemental maps of the steel/Cu interface</i>	63
<i>Figure 40: Scheme of the laser texture procedure</i>	65
<i>Figure 41: Images of laser textured steel samples (1.5 x 1.5 x 2 mm)</i>	66
<i>Figure 42: Top view FESEM images of the surface treated steel samples</i>	67
<i>Figure 43: EDS spectrum of sample 1</i>	68
<i>Figure 44: EDS spectrum of sample 2</i>	68
<i>Figure 45: EDS spectrum of sample 3</i>	68
<i>Table 1: Chemical composition (Max. value) of AISI 316L and EUROFER 97</i>	50
<i>Table 2: Chemical composition at Cu/steel interface</i>	57
<i>Table 3: Weight and atomic concentrations of sample 1 (EDS)</i>	65
<i>Table 4: Weight and atomic concentrations of sample 2 (EDS)</i>	65
<i>Table 5: Weight and atomic concentrations of sample 1 (EDS)</i>	65

ABSTRACT

This work is framed in the joining technologies for fusion reactor applications, more specifically in ITER tungsten-to-steel joints. The main problem for W/steel joints is the mismatch between the coefficients of thermal expansion of tungsten and steel that after joining process causes residual stresses at the interface, reducing the strength of the whole joint. Moreover, the deeper diffusion of the metallic filler (in case of brazing) leads to a softening in the seam area and consequently has a detrimental effect on mechanical properties. Finally, the direct contact between copper and steel causes the formation of a reaction layer constituted of brittle compounds which weaken the whole joint.

This thesis is divided in two parts, one regarding bibliographic research in which different kinds of nuclear fusion joints are described, and a second one which is experimental and was carried out at Politecnico di Torino within the Glance Group (Glasses Ceramics and Composites). The joints have been manufactured using a brazing process, based on pure Cu or commercial Cu-based filler (Gemco®); analysis have been performed on W/Cu/steel and W/Gemco®/steel joints, and on a possible surface modification of the steel by laser, in order to improve the joint performance.

Following a complete bibliographic research, different brazing conditions were analysed, to find the optimal parameters to achieve sound W/steel joints. The brazing technique seems to be one of the most suitable for ITER joints, thanks to its easier applicability and well-known technology. The first activity is focused on brazed joints, and two studies are carried out. First, a W/Gemco®/steel joint is produced, in order to investigate if the presence of a Cu-based alloy as filler material (87.75 wt% Cu, 12 wt% Ge and 0.25 wt% Ni) reacts well with the adjacent base materials, considering the ductility of Cu and low-activation of Ge. W/Cu/steel joint has been investigated as well. Moreover, we proposed a way to reduce the diffusion of the copper inside the steel, adding a thin Cr layer on the surface steel substrate. The layer was deposited on the steel samples by magnetron sputtering technique, in order to create a barrier for copper diffusion. For the same reasons, a coating of Cr was also deposited on the steel surface of the W/Gemco®/steel joint. Joints manufactured with and without Cr coating have been compared. The microstructures and the chemical compositions were characterised by Field Emission Scanning Electron Microscopy (FESEM) analysis and with Energy Dispersive Spectrometry (EDS) technology.

Finally, the produced joints will be subjected to High Heat-Flux tests at Forschungszentrum Jülich Research Centre (FZJ- Jülich, Germany) and eventually to

mechanical tests. The second activity is centred on a modification of the steel surface, in order to prepare the steel face for direct bonding with tungsten improving its mechanical and tribological properties.

Three steel samples were characterised and textured with a nanosecond laser, varying the laser power and fluence. The aim of this thesis is to produce a good starting point for the manufacturing of W/steel joints, with improved performance if compared to joints manufactured by direct bonding, and to demonstrate that the presence of Cr on the steel surfaces of brazed joints may represent a promising solution for fusion nuclear joints. However, further investigations are needed, and a thermo-mechanical analysis must be explored.

INTRODUCTION

It is known that the international scientific community is focused on the development of new and innovative technologies to produce thermal and electric energy minimising costs, emissions, and energy consumptions. That said, the focus has shifted on the generation of power by non-conventional sources as nuclear fusion energy that, thanks to its characteristics and to the low production of nuclear waste, can be considered as one of the most promising technological solution.

In relation to this project, the international scientific community is developing the *International Thermonuclear Experimental Reactor (ITER)*, a nuclear fusion facility under construction from 2007 in Caradache (France), which will have to demonstrate the engineering and technological feasibility of fusion power providing an output of 500 MW.

The extreme operating conditions that these kinds of power plants (*Tokamak* type) can reach make it necessary to consider different aspects, in particular three main challenges from an engineering point of view. The first one consists of exhausting the power generated by alpha particles whose main purpose is to heat the plasma (up to 20% of the fusion power) that, being deposited, must be transmitted to material surfaces [1]. These faces can be in principle both, divertor surfaces or surfaces facing the main plasma [1]. The second technological challenge is the one referred to the confinement of plasma with a temperature of 10^8 K using superconducting magnets that must be kept at 4.5 K. The last one is related to the extraction of the power deposited in the blanket by neutrons through a cooling system and the capability of the blanket to breed the tritium. In fact, the plasma facing components, being subject to very high heat fluxes and loads due to the emission of neutrons with an energy spectrum whose peak value is 14 MeV, can physically and mechanically wear down modifying their properties and, consequently, compromise the integrity of the structure itself.

The emission of neutrons and the flux generated by Deuterium-Tritium reaction are of the order of $10^{18} \text{ m}^{-2} \text{ s}^{-1}$ and they lead to an important reduction of component's life caused by the degradation of metals properties (e.g. ductility) and by a decrease in energy efficiency of the system. Moreover, the formation of heavy nuclei due to the D-T reaction and the high concentration of reaction products such as He or H, induce a phenomenon called *swelling* which is characterised by the formation of porosity and a consequent reduction of the material density.

The presence of surface heat flux due to this neutron and particle flux coming from the plasma, which is at temperatures of the order of 100 million degrees, is of particular

interest because the thermal load may be such as to achieve orders of MW/m^2 for the *Plasma Facing Components* (PFC). ITER *blanket* and *divertor* are PFC in fact, their parts are subjected to heat flux of the order of $4,700 \text{ kW/m}^2$ and $20,000 \text{ kW/m}^2$ respectively.

The blanket is the first component beyond the *First Wall* (FW) and its main functions are linked to extract the power deposited by neutrons and to shield, with *Vacuum Vessel* (VV), the magnets outside. The divertor component is positioned at the bottom of the plasma chamber. It has the purposes to exhaust most of the alpha particle power and to eliminate impurities from the plasma because its performance is affected by the transport of the latter.

As a consequence, it is simple to understand that this mission requires a thorough knowledge of material's components because they are subject to very high energetic neutrons whose flow is orders of magnitude greater than that achieved in nuclear fission plants.

Different aspects touch the choice of PFM (*Plasma Facing Materials*) such as the tritium inventory and co-deposition, the surface offered for heat removal, the volumetric heat deposition, and mostly the radiation effect from neutrons and edge alpha particles. For these reasons, Beryllium has been selected for the FW and Tungsten for divertor.

The neutron damage is an important aspect to analyse because it is the main lifetime limiting phenomenon for a nuclear fusion reactor. It is measured in dpa (*displacement per atom*) that gives a sort of measurement of quantitative neutron damage and, according to the neutron spectrum energy, it is related to the changes and modifications in the macroscopic properties of materials [2]. The dpa is proportional to neutron fluence (obtained multiplying the wall load by the plasma burn time) which is strongly dependent on radiation effects as nuclear transmutations, variation of defect concentration, helium bubbles production, embrittlement. The irradiation damage measured reaches values up to 150 for blankets and up to 50 dpa for divertor.

In order to increase the reliability of the system, to have an intrinsic safe and adaptable design, the fusion community is working hard to reduce and simplify each component. According to these needs, ITER FW presents a modular structure, made with modules distributed both in toroidal and poloidal directions that present an assembly of tiles. In this way it is possible, in case of rupture, a relatively easy maintenance and a fast substitution.

Certainly, the current high temperatures involve the use of different materials that must be joined with each other, which represents a big challenge for fusion devices because different materials imply dissimilar mechanical and physical properties and consequently many types of joints.

CHAPTER 1

JOINING TECHNOLOGIES

1.1 ITER technologies

The realization of ITER machine and its components requests a precise and careful work. To do that, some prototypes are being developed and constructed for decades, in order to demonstrate their feasibility. ITER includes a series of components of which the main ones are: Tokamak, Magnets, Vacuum Vessel, Cryostat, Blanket and Divertor.

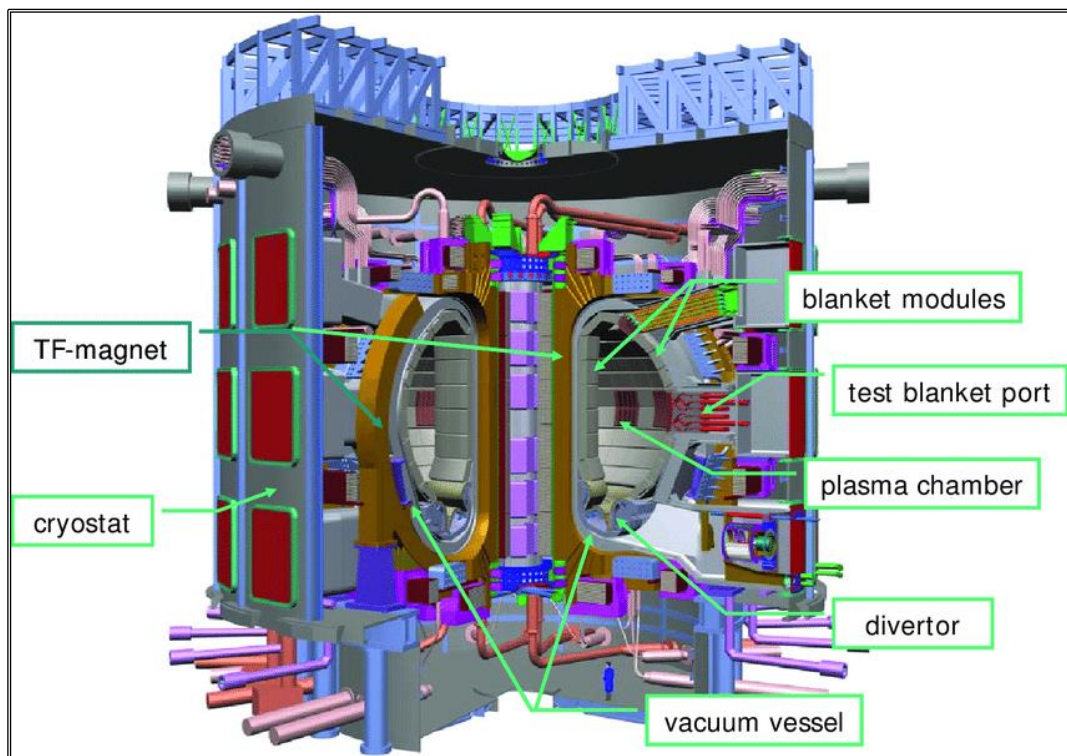


Figure 1: ITER structure [3]

The Tokamak design is a toroidal type of plasma confinement in which three components of a magnetic field are involved to control and limit the plasma inside a characteristic doughnut-shaped vacuum chamber. To initiate the process, all the air and the relative impurities are removed in order to obtain vacuum condition. After that, the magnetic field coils are charged and, at the same time, the fuel is led inside the vacuum chamber. When the conditions are optimized, a very high current is run through the vessel, the gaseous fuel particles are electrically ionized and form the plasma [4]. As the charged particles are flowing and tend to go towards the wall, a system of auxiliary heating helps

the plasma to reach fusion temperatures (over 150 million °C) in order to overcome the electromagnetic repulsion forces between particles. Meanwhile the magnet act as control and shape system, leading the plasma away from the walls of the vessel. ITER will be the world's largest tokamak, with a plasma radius of 6.2 m and a plasma volume of 840 m³ [4].

The Magnet structure of ITER is composed by 18 *toroidal field coils* (TF), 6 *poloidal field coils* (PF) and 6 *central solenoid coils* (CS). This superconducting system will produce the magnetic field mentioned before that will confine, control and shape the plasma. The magnets are manufactured with Nb₃Sn and NbTi and they become superconducting at 4.5 K, when they are subjected to supercritical helium at cryogenic temperature. These superconductors must carry high currents and magnetic fields, hence, in order to have high performances, *cable-in-conduit conductors* (CICC) are used. They are made with thousands of strands, mixed with copper for stability, all cabled together and everything is embedded in a *jacket*. The fragmentation of the filaments is due to the fact that there are AC losses as consequences of the fact that ITER is intrinsically a machine that is not operating in steady state condition. Besides, there are also hysteresis losses that are proportional to the cross-section of the superconductor. For this reason, the dimensions of the elements are minimised (order of micro-meters) twisting all the strands around the central spiral (*twisted shape*).

As said before, there are three components of magnetic field. The main one is the toroidal field along the torus axis that is generated by a set of D-shaped TC spaced around, that produce a maximum magnetic field of 11.8 T [5]. Due to the fact that TC are subjected to very high forces the fusion community decided to use the Nb₃Sn (it resists to higher value of magnetic field with respect to NbTi) as material for superconductors, placed in special radial plates with a “double-pancakes” configuration. The overall structure is encased in a structure of stainless steel. However, the toroidal magnetic field is not sufficient to confine the plasma because in toroidal geometry a combination of forces, including the plasma pressure, arise and tend to push the plasma towards the walls. In order to reach the equilibrium between the particle’s drift (plasma pressure) and the magnetic forces, the poloidal magnetic field is taken into account. It is produced by the current circulating inside the plasma itself and the PC, that are located outside from the toroidal structure and are made of NbTi, provide to stabilize the plasma far from the wall and they are subjected to a magnetic field of 6 T as a maximum. The combination between the toroidal and poloidal components of the magnetic field, creates a helicoidal shape of magnetic field lines inside the torus. Finally, there is the vertical field whose purpose is to provide suitable shapes of the magnetic surfaces because they affect the stability of the

system. The CS packs allow the induction of a powerful current of 15 MA for a duration of 300-500 seconds [5].

The *Vacuum Vessel* (VV) is made by a double wall of stainless steel that allows the flowing of the cooling water that will remove the heat produced during operating conditions. It shows different functions; it constitutes the first primary confinement for radioactivity [6], therefore it provides safety inside the system. It must withstand to the magnetic and heat loads due to the particles flowing inside of the plasma that can undergo to plasma disruption and eventually, during an accident, it has to maintain the vacuum inside without losing the confinement. Furthermore, it provides an important neutron radiation shielding for the magnets and for the structural materials outside of the vacuum chamber. The VV is also equipped of forty-four openings (windows/ports), that allow an easier remote handling for maintenance and diagnostics, and permit the heating of the system.

The Cryostat is a cylindrical, fully welded, vacuum chamber made with stainless steel that has to tolerate a pressure vacuum of 10^{-4} Pa [7]. It represents an important support for the system because it suffers all the mechanical loads due to the gravity, electromagnetic forces and expansion or contraction of the components. Therefore, the cryostat presents 23 penetrations for maintenance and more than 200 for diagnostic, the removal of some parts of the blanket and divertor and, the auxiliary heating [8]. Furthermore, the design of the overall system requires a cryostat with a removable part on the top to consent, in case of need, the removal of CS [7]. Finally, the bottom central part is welded with the main cylinder in order to support the entire assembly.

The blanket covers all the inner vacuum vessel walls and it is the components which delimits the plasma region from the rest of the system. It is made of 440 modules distributed both toroidally and poloidally that are assembled in such a way that it is possible to identify “sectors”. These sectors are the ones that host the ports, useful for maintenance. The blanket modules protect the entire structure outside including the superconducting magnets because during operation there is an important production of heat that has to be removed and there is also a dangerous neutron irradiation for magnets that can lead them to a reduction of performances. Each sector is made with 4 modules inboard, 4 modules up and 8 modules outboard. From figure 1 it is possible to notice the fact that they are shaped in such a way to make easier the maintenance, because the FW modules will be replaced at least, once. The blanket is one of the two PFC that faces directly the plasma, so it has to exhaust a big part of its power. It is subjected to a non-uniform heat

flux according to the panel position in fact, two different kinds of FW panels have been developing: the FW normal heat flux panels for heat fluxes up to 2 MW/m^2 and the enhanced heat flux panels for values up to 4.7 MW/m^2 [9]. Besides, the blanket system comprises also the blanket manifolds, which route the coolant to the blanket modules [13].

The divertor aim is to minimize the problem of impurities and ashes that travel within the core plasma. Neutral particles are intrinsic parts of the plasma edge region so they must be pumped away in order to maintain the high vacuum conditions (0.1 Pa) inside the machine and to try to make the plasma as pure as possible (ideally D-T only). It is situated in lower part of the plasma chamber and it is made of a supporting structure composed by a *cassette body* (54 assemblies) that is extended all around toroidally and, of different components that may interact directly with the plasma. The inner vertical target, the outer vertical target and the dome in fact, are in direct contact with plasma particles and neutrals. Neutrals, have to be pumped by an external pumping system and, to guarantee a good environment for the pumping of neutrals, the baffle regions are shaped in such a way to have high pressure at the inlet of the pump. Moreover, the presence of the reflector plates makes possible the recombination and re-immision of particles that escape from the plasma and similarly the dome helps to get back particles into the plasma. The part between the inner and outer divertor is not impermeable for neutrals, so that they can travel from one vertical target to another creating a recirculation that leads to a reduction of the heat load for the target. The following figure shows a representation of the divertor components.

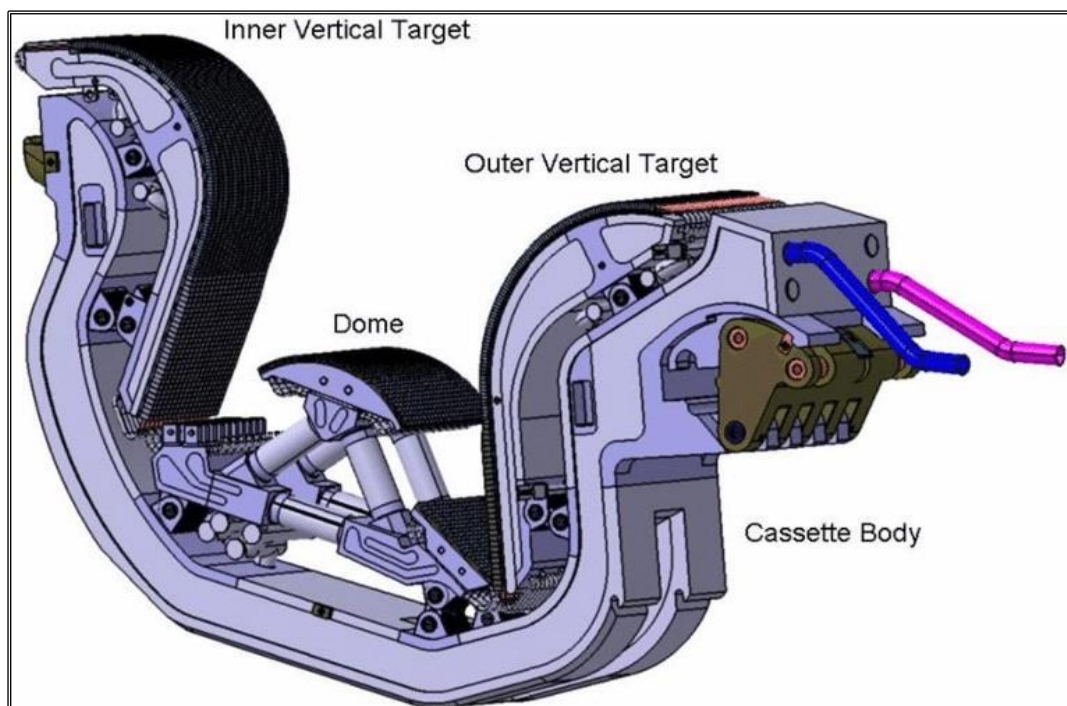


Figure 2: Divertor structure [10]

1.2 PFCs materials and configurations

ITER components are characterised by different temperatures and radiation damage, but irradiation effects on Plasma Facing Component are crucial, therefore, a careful choice of materials is needed.

Typical effects of neutron damage are connected to the reduction and modification of chemical, physical and mechanical properties. Nuclear activation makes the material radioactive, the embrittlement of the material, due to the production of He, causes the welding more difficult and the loss of thermal conductivity gives rise to a reduction of the heat removal capacity. Moreover, the particle flux coming from the plasma starts a phenomenon known as *sputtering*. The process consists in a surface erosion by particles that hit the first wall, causing a progressively decrease of Plasma Facing Materials (PFMs) thickness and, if the wall is saturated, the eroded particles can migrate into the plasma causing radiative energy losses.

To avoid these effects, and to reduce the plasma instabilities that may lead to an instantaneous deposition of heat into the PFCs, a materials combination for plasma-facing components is necessary. In general, in order to withstand to surface heat fluxes a material with a high melting point and thermal conductivity is required. Furthermore, a material at low activation is needed for neutron irradiation and with low atomic number to reduce and limit the bremsstrahlung losses.

The fusion community is working on a design strategy which consists of different configurations and materials. For the structural materials it is important to control the content of Ta, Co and Nb in order to reduce the activation of material and the concentration of B to limit the production of He, which leads to the material He embrittlement [11]. Moreover, a large temperature window is required for the compatibility with coolant and functional materials: high range is limited by a reduction in strength and formation of creep and low range is limited by the Ductile to Brittle Transition Temperature (DBTT).

In ITER, the main structural material for PFCs is *austenitic stainless steel* (316 type). It is used in many engineering areas as it presents adequate mechanical properties, good wettability, it is available in different forms and has a good resistance to corrosion environment. As armour materials, *tungsten* (W) and *beryllium* (Be) are the candidates. The first one has been chosen for divertor because it presents suitable characteristics and good compatibility with high heat loads. Tungsten presents a high melting point (3400 °C), a good thermal conductivity (174 W/mK), as well as low sputtering yield that indicates how many atoms of W enter the plasma per deuterium ion hitting the wall and, a low

tritium retention that is important for the fuel economy. Besides, due to the fact that divertor is the part in which the heat flux has the higher value, tungsten can be a good choice also for its high-thermal stress resistance. However, there are some non negligible disadvantages, such as poor machinability, a high atomic number (Z) which causes a low concentration of W particles inside the plasma allowed, a high radioactivity and, it shows an explosion dust potential.

The second material is *beryllium* that is used in the blanket. In particular, it is the element that covers the FW, the rest of the blanket structure is made with stainless steel and of high-strength copper [9]. Its interfacing to the plasma is due to the fact that it presents a low atomic number and it is not exposed to chemical sputtering, so as enhance the plasma compatibility. Also, beryllium is a low activation material, characteristic that is fundamental for neutron irradiation, and exhibits a high thermal conductivity (200-500 W/mK). As tungsten, it has disadvantages because it presents a relatively low melting point (1287 °C) that leads to a small erosion lifetime and, from a neutron irradiation point of view, its behavior is characterised by swelling.

Between the cooling channels and the armour is placed the heat sink, a fundamental part for the entire structure because its main function is to make the heat exchange as easier as possible, reducing thermal stresses. This stress reduction is done thanks to the capability to transport the high heat generated inside the machine to the cooling channels in which water is flowing. For the heat sink pure copper would be the principal choice in principal for its high thermal conductivity (390 W/mK). Unfortunately, it is very sensitive to radiation damage and shows an important reduction of the strength at moderate temperature.

The *Copper-Chromium-Zirconium alloy* (CuCrZr) has been chosen as heat sink materials because it presents enhanced mechanical properties, a high thermal conductivity (>300 W/mK), its weldability has been verified and a significant amount of data for the CuCrZr alloy (0.6-0.9 wt%Cr, 0.07-0.15 wt%Zr) is available in databases [11].

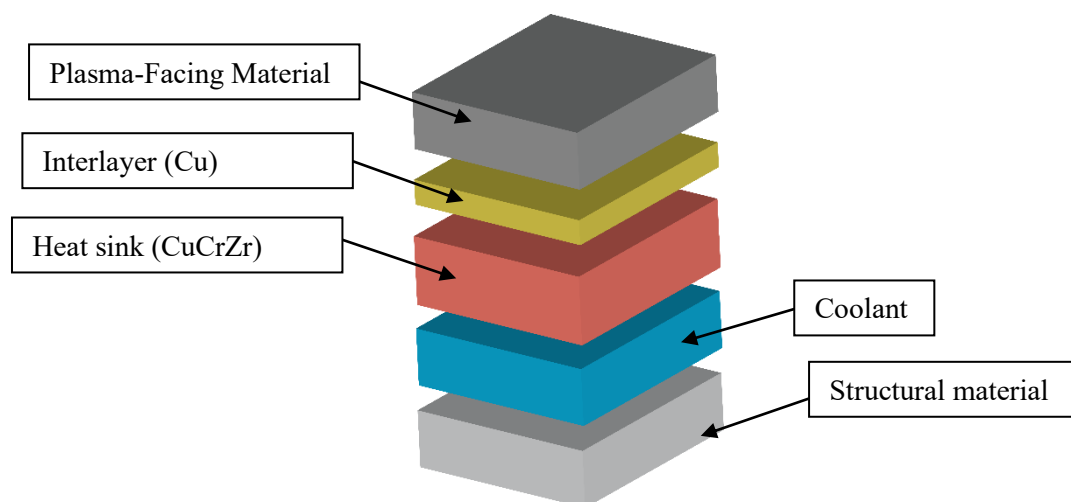


Figure 3: PFCs material combination

As the figure 3 illustrates, a generic part of plasma-facing component combines different types of materials. Focusing on the top, there is an interlayer made of copper between the plasma facing material and the heat sink. This is because the coefficients of thermal expansion of the two materials are different thus, in order to avoid thermal stresses, the pure copper interlayer accommodates, by plastic deformation, the thermal expansions minimizing the dissimilarities. From a design point of view, according to the intensity of the heat flux, different configurations have been chosen. The blanket is composed by the *first wall panels* and the *shield blocks*. The first ones are detachable and made with beryllium tiles bonded with CuCrZr and stainless steel [9]. Furthermore, these panels present a “fingers” shape that is attached to a structural beam which host the water coolant channels [9]. The shield blocks are lock at four points with the vacuum vessel, and their main purposes are to shield properly the magnet system and the vacuum vessel.

The divertor design shows three patterns: the *smooth tube*, the *hypervapotron* and, the *twisted tape*. The first two belong to the *flat tile* configuration, that is easy to manufacture but not highly resistant to cyclic loads. The twisted tape configuration appertains to the *monoblock* design which instead presents very good resistance to cyclic loads. Also these configurations have been assigned with respect to the intensity of the eat flux received. For heat fluxes $< 3 \text{ MW/m}^2$ the smooth tube design is used, for heat fluxes $> 10 \text{ MW/m}^2$ the monoblock design with twisted tape in the coolant channel has been chosen. As the figure 4 shows, in the divertor dome as well as in the reflector plates, the hypervapotron configurations is used for heat fluxes in a range of $3\text{-}10 \text{ MW/m}^2$. The structure is made with tungsten tiles supported by a pure copper layer which in turn is resting on the CuCrZr heat-sink that presents the hypervapotron configuration. This design is useful for the fact that, due to the presence of cavities in which the fluid is forced, the rotation of this fluid increases the turbulence and leads to the formation of secondary flows which in turn improve the heat transfer capability of the system.

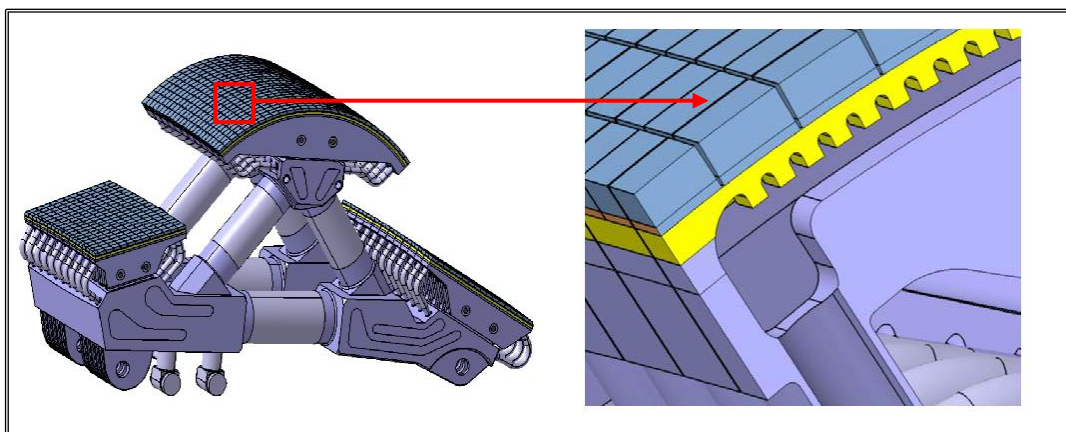


Figure 4: Dome hypervapotron design [11]

1.3 Joining requirements

Plasma Facing Components must be joined with ITER structure and the variety of materials involved leads to discontinuities and mismatches between their mechanical, chemical and physical properties. As a consequence, the joints have to satisfy different requirements which unfortunately are not well established yet.

During reactor operation the temperatures and the high heat fluxes may lead to significant changes in the microstructure of materials. For this reason, the joint should be mechanically and thermodynamically stable up to temperatures of 800 °C. For example, considering a joining between W and Fe, the maximum temperature of the former should not overcome 1200°C due to recrystallization and the maximum temperature of the latter should not exceed 650°C for the onset creep; consequently, the maximum temperature of the Fe/W joint must not rise above 800°C due to some creation of intermetallic phases, for short durations of operations only [12]. As said before, it is also necessary to work with materials that present high thermal conductivity during the operation and high thermal shock resistance.

The stability of the joints is related to different aspects. The joints operate under vacuum conditions and, the combination with neutron, mechanical and thermal loads require a focused design, because they must survive under stress operations. The joints also must provide an acceptable reliability under cyclic mode in order to offer a long design lifetime ensuring a suitable cost of the overall components.

Besides, the neutron-induced radioactivity is an important phenomenon that implicates the choice of joining materials preferably with low activation characteristics. The *Low Activation Materials* (LAMs) in fact, minimise the radioactive content and emission of the components during normal and off-normal conditions leading to a safer nuclear environment (i.e during maintenance) for workers and for population. Moreover, the use of these kind of materials is important for waste disposal.

Finally, to preserve the joints features, it is fundamental to have a deep knowledge of the properties of the materials involved because in some manufacturing process the thermo-mechanical characteristics of the joints may change and lead to the failure of the joint itself. Some materials in fact, are not compatible with the brazing joining technique which may implicate neutron transmutations or poisoning of some components and, the different coefficients of thermal expansion may create thermal stresses exactly in the joint area, which can be considered as the “weaker” part of the component.

1.4 Joining for ITER

The success of ITER will lay the foundation for the future fusion reactor known as *Demonstration thermonuclear reactor* (DEMO) characterised by higher heat fluxes and neutron irradiation. For these reasons, the structural material adopted will not be the austenitic stainless steel but the low activation ferritic-martensitic steel EUROFER97.

In the nuclear fusion frame, for both reactors, one of the most difficult challenge is related to the joints of tungsten with steels. The realization of these connections is hard due to the differences in their physical properties. The main problem shows up especially at high temperatures, when the expansion of the two materials increases and the mismatch between the coefficient of thermal expansion is more evident (CTE $4.5 \times 10^{-6} \text{ K}^{-1}$ for tungsten, $12.7 \times 10^{-6} \text{ K}^{-1}$ for EUROFER97 [14], and $15.0\div 16.5 \times 10^{-6} \text{ K}^{-1}$ [15] for austenitic stainless steel). In fact, when the joined materials are cooled down, from the joining temperature to room temperature, higher residual stresses characterise the interface of the joint.

Currently, different joining procedures are involved in the fusion field:

- Diffusion bonding;
- Brazing using interlayers (foils), powders or liquid-forming interlayers [16];
- Steels surface treatment modifications;
- Functionally grade materials interlayers.

Nowadays, brazing and diffusion bonding methods are considered the most suitable to construct strong and reliable joints for divertor and FW components.

The diffusion bonding is characterised by two pieces (to be joined) kept in close touch for a certain amount of time, with high temperatures and moderate pressure. This technique takes into account the phenomenon related to the solid state diffusion, in which atoms diffuse from one material to the other creating a bonding. During the stages of the process the surfaces deform, they get in contact, and atoms, starting to diffuse, causes a rearrangement of the grain boundaries which in turn reduce the pores at the interface [18]. The bonding temperature is important for diffusion phenomenon and the consequent reaction layer/product formed. In fact, if the bonding is made with similar materials only one phase is formed in the diffusion zone; if the materials are too much different more intermediate phases will form [18] and due to the fact that they are commonly brittle, may lead to a reduction of the strength of the joint.

Usually, diffusion bonding is performed by hot isostatic pressing (HIPing) and spark plasma sintering. The first technology includes high temperature and gas pressure in order to create a material with isotropic properties. It is widely considered because, thanks to its characteristics, it is possible to join dissimilar materials with curved shapes and large surfaces obtaining at the same time enhanced material properties and reduction of pore defects [19].

The second method known as spark plasma sintering (SPS) consists in a pressure-assisted pulsed-current process [20] in which samples are sintered in uniaxial pressure. In particular, the sampling is subjected to a pulsed DC that passes directly through it allowing an internal heating by mean of an external source. This permits to obtain a final product with a reduced pore density in a small time (the process is very fast).

The brazing technique is based on the joining of two or more parts, melting the filler material, located between them. It is a discontinuous joint, it can be used to join different materials, it presents a low cost process, and ensures a reduced thermally altered zone in the joint area. In order to have a successful brazing the melting temperature of the filler must not exceed the one of the two base materials to be joined. In this way the liquid, due to a capillary action, can penetrate exactly the region at the interface and then, when it is cooled, provides a strong joint between the base materials generating an intermediate layer which guarantees a continuous joint [17].

In order to achieve a strong bonding, a direct modification of the metal surface may be necessary. Laser surface treatment has been developed to enhance the tribological and mechanical properties of the joints. Being a localized treatment, lasers allow to modify different substrates in different zones: in fact, according to the requirement of the joint, the surface can be altered only in one region with respect to the entire surface. Moreover, it is also possible to treat complex shapes. Another important aspect is related to the strength of the bonding: the laser texturing surface improves the roughness of a metal and in this way, likely, the wettability of the joined area is enhanced and the surface area is increased. If applied to a metal surface, the laser texture patterns influence the surface morphology of the material improving its adhesion and, consequently, its mechanical properties as the tensile shear strength, stress resistance, and adhesion.

According to the nuclear fusion environment, the materials involved in ITER, in particular in the FW or in divertor, are subjected to very strong modifications. As said before, the mismatch between the CTE of tungsten and steel is one of them. In order to reduce the residual stresses at the interface of the Steel/W joints *functionally graded materials* have

been developed (FGMs).

FGMs generally are made of two materials [21] which are industrialized in such a way to distribute, gradually, the fractions of the two constituents. The gradual spatial dissimilarity in the microstructure leads to a smoothed distribution of the mechanical and thermal characteristics of the two materials involved allowing to have better performances.

Steel/W composite materials have been improved and fabricated in different ways, in particular with atmospheric and vacuum plasma spraying (APS and VPS), and electro discharge sintering (EDS) [22].

CHAPTER 2

TUNGSTEN-STEEL JOINTS

2.1 Diffusion bonding

The joining of tungsten and steel is one of the most challenging engineering concept in the nuclear fusion field. Several joining techniques have been developed in the last years, taking into account the chemical-thermal-mechanical properties of the materials involved.

Diffusion bonding (direct) was the first approach for joining considered, due to its well-known technology. In fact, during the application, only the base materials are used and the joining is made in one step. The process can be carried out in different ways: with and without post bonding heat treatment, with single and two step uniaxial diffusion welding, with spark plasma sintering (SPS), and with Hot Isostatic Pressing (HIP).

In the case without Post-Bonding Heat Treatment (PBHT), W. W. Basuki et al. [23] experimented the W/steel joint with different bonding durations (1h, 3h, and 4h), and the diffusion bonding was performed at 1050 °C. The experiments showed the formation of two layers in the joint seam region, containing intermetallic phases and carbides (likely brittle) which may led to a weakening at the direct bond interface area. Besides, the heat treatment did not eliminate the residual stresses at the bonding face, reducing consequently the mechanical properties of the base material.

In [24], the results show that it is reasonable to produce a good joint with one or two uniaxial-direct welding but the latter process demonstrates that the two steps method has a very important advantage: it reduces the compression and the consequent deformation of the sample. Nevertheless, the subsequent heat treatment is responsible for alterations in tensile properties and for an increasing failure at the base material for the tensile strength.

For the FW applications, it is preferable to have a joint as simple as possible. To obtain it, SPS and HIP were used to avoid the degradation of the braze material under neutron irradiation, in the case of brazing [25]. Results showed that the second process could be better with respect to the second but the formation of oxide on the surfaces of the joint made it not so adequate.

The direct joining of W and steel/EUROFER has not been successful in the last years. The direct bonding, in fact, presents times and processes not as convenient. The temperatures and pressures used are very high and the base materials involved may be

affected and characterised by the onset of distortions and/or cracks. Moreover, only flat parts can be joined and this makes the diffusion bonding a non-flexible technology. For these reasons, a deeper and focused study is necessary, in order to find the right parameters and to experience new joining methods.

2.2 Diffusion bonding by HIP

In order to improve the joining strength, the insertion of interlayers between the base materials during HIP could represent a good solution.

Yang-Il Jung et al. [26], experimented a W/Steel joint using Ti foils as interlayers. They performed the HIP procedure in two steps: the first at 900°C with a pressure of 100 MPa for 1.5 h, and the second at 750 °C, 70 MPa as pressure for 2h (in order to re-establish the mechanical properties of the ferritic-martensitic steel). The final results showed a good bonded joint with a continuous interface and free of defects.

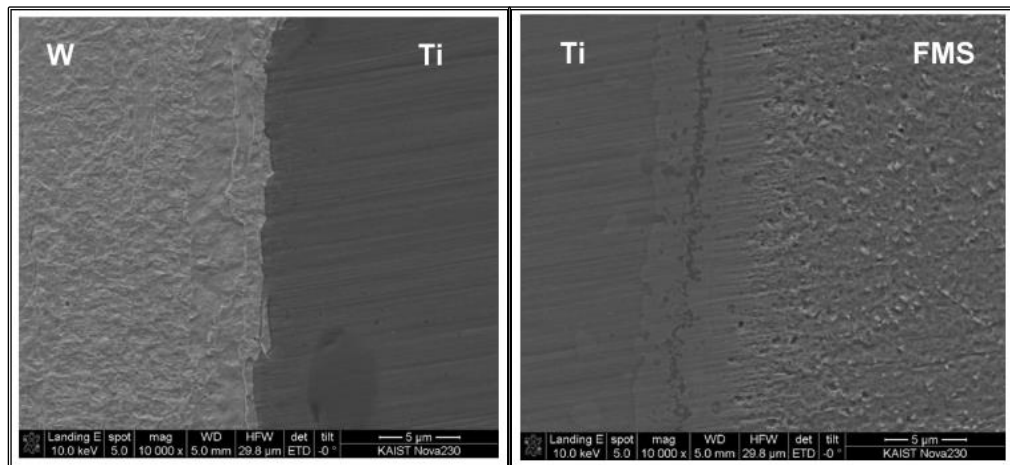


Figure 5: SEM images of W/Ti and Ti/FMS interfaces [26]

Nevertheless, they did not demonstrate the presence of a brittle fracture, so it is possible to refer to the work of Ji-Chao Wang et al. [27], in which the authors tested different samples of W/Ti/316 stainless steel joints at the following HIP conditions: 930°C, 100 MPa, for 2 h. More in details, from their experiments emerged that using interlayers of Ti >100 μm, the formation of intermetallics compounds significantly reduced.

In particular, they joined successfully the samples observing a free W/Ti interface from intermetallics, and then some reaction compounds as TiC, FeTi, and Fe₂Ti₄O at the Ti/steel interface. Besides, from the shear strength point of view they found 140 ± 5 MPa, 127 ± 7 MPa, 139 ± 12 MPa for 100, 300, and 500 μm respectively, higher values than [28], considering 151 MPa as maximum value.

In addition, from fig.6 it is possible to observe the fracture of the specimens with 100 and 300 μm as thickness of Ti, in which some brittle phases are highlighted and that, probably, are the responsible for a brittle fracture.

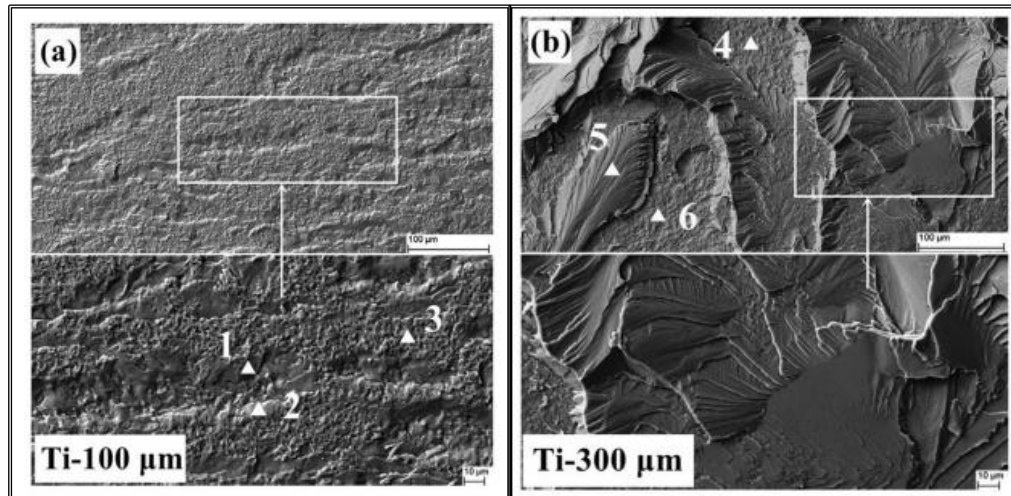


Figure 6: Fracture surfaces of W/Ti/steel joints with a) Ti-100 μm , b) Ti-300 μm [27] as joining interlayer

Further investigations have been developed during the years as concern the use of Ti as interlayer. Wensheng Liu et al. [29] created a W/steel joint using a Ti/Cu/Ti liquid forming interlayer in order to improve the strength of the joint even with a significant roughness. They obtained a well bonded joint making the HIP at 1050°C, 100 MPa, for 1 h [29]. In particular no cracks or unbounded regions were detected.

Even in this case the use of Ti as interlayer is not free of disadvantages because a reaction layer at the Cu/steel interface was detected, containing brittle compounds as TiC, TiFe, TiFe₂, and TiCr₂. This last part, having a hardness of 18.6 GPa, constituted the weakest region of the joint.

Ji-Chao Wang et al. [30] tested the quality of a W/Ti/steel (FMS grade 91) subjecting it to deuterium exposure at different partial pressures. The interlayer material was a Ti interlayer of 0.5 mm thickness, and the HIP process was carried out at 760°C, and 150 MPa for 4 h [30].

The experiment showed different results according to concentration of D₂ and to its partial pressure. In general, the authors obtained a good joint, well bonded and free of voids or defects, as the previous investigations demonstrated.

The fig. 7 shows the W/Ti and Ti/steel interfaces after the HIP, before the D₂ exposure, and after. The Ti interlayer total disintegrated with partial pressures that go from 200 to 1000 Pa. Moreover, under the same conditions with a low concentration of deuterium, it is noticeable that small structures formed at the Ti/steel side.

Instead, with high concentration of D_2 the joint could undergo to the creation of $Ti D_2$ which, sooner or later, may lead to a failure of the whole joint.

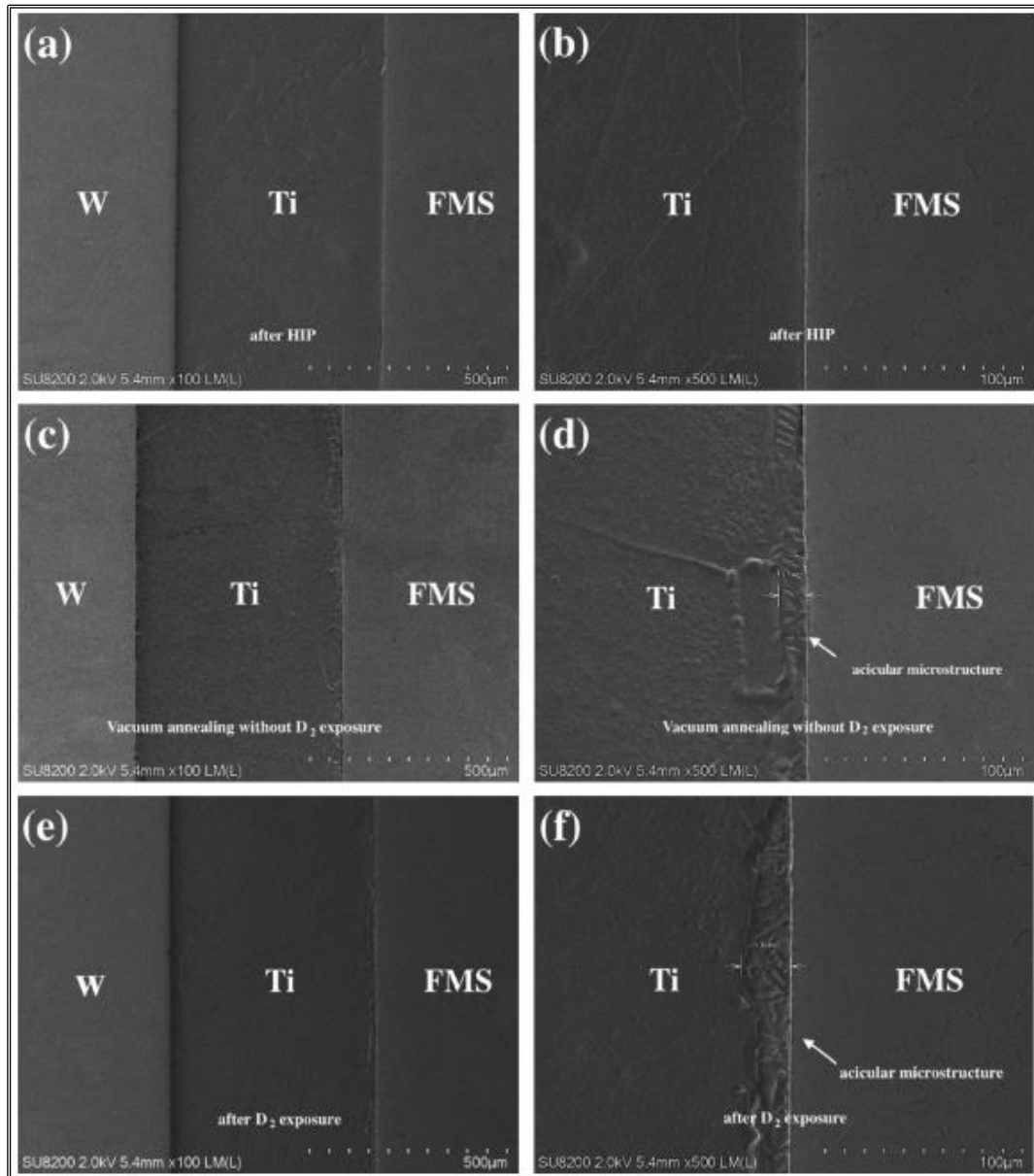


Figure 7: SEM representations of the joint a-b) after HIP, c-d) after vacuum annealing with no D_2 , and e-f) after deuterium exposure with a partial pressure of 1000 Pa [30]

From this experiment, the authors demonstrated that the response of the materials joints changes according to the concentration of deuterium. If the amount is low, the presence of D may be beneficial to the strength of the joint thanks to the increased diffusion of elements. Besides, the presence of D may decrease the yield stress of titanium, leading to a better capability of accommodate the residual stresses during cooling [30].

On the other hand, if the concentration of deuterium is high enough the bonding strength can be reduced for hydrogen embrittlement because of microstructure modifications. As a conclusion, due to the fact that the nuclear environment is widely

subjected to hydrogen embrittlement, it is important to establish some threshold values beyond which the formation of hydrides may lead to the joint failure. As in case of titanium as filler materials, other studies were performed with different materials as interlayers. Yang-II Jung et al. [31], used a zirconium foil of 25 μm as interlayer to join W with FMS. They performed a two steps HIP process. The first stage was carried out at 950°C, with 100 MPa for 1.5 h. The second one at 750°C, with 70 MPa for 2 hours.

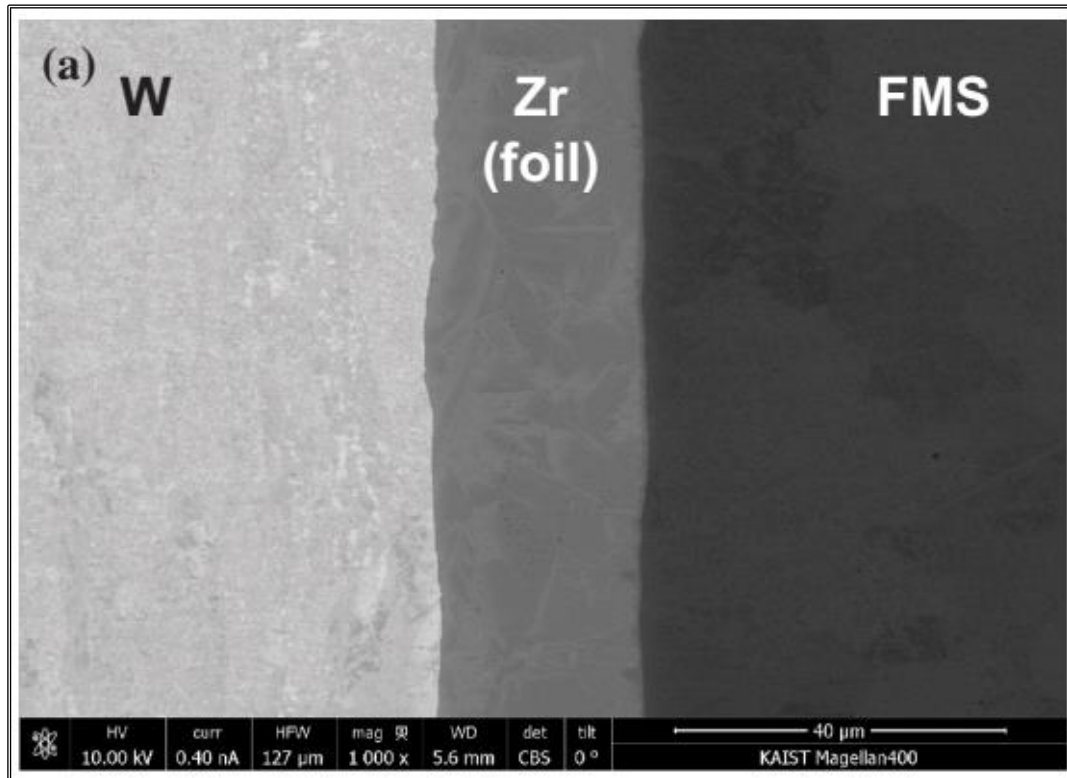


Figure 8: SEM image of the W/Zr/steel joint [31]

As fig. 8 shows, at low magnification the joint did not present any type of defects, voids, or pores. At higher magnifications, it is possible to observe that in the W/Zr side of the joint there were no defects and just a thin layer was formed (150 μm).

On the other side, the Zr/FMS part, the presence of Zr-W compounds has led to think

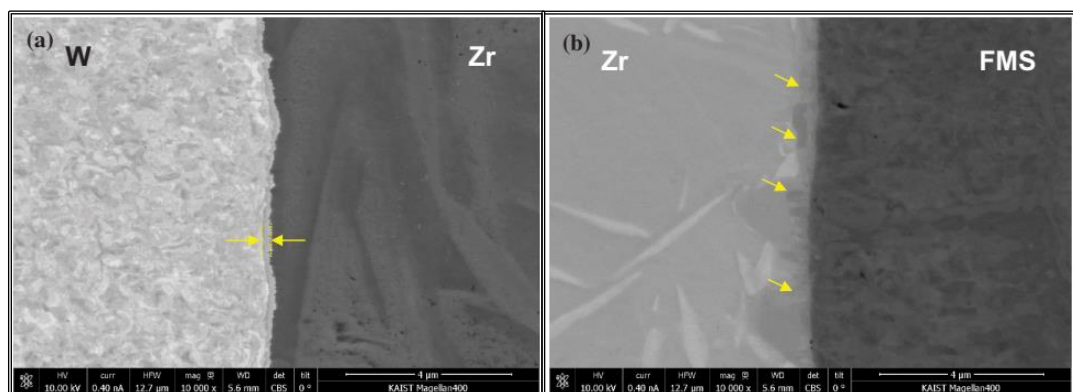


Figure 9: SEM images of W/Zr and Zr/steel interfaces [31]

that these intermetallic phases may be the responsible for a brittle failure of the joint.

However, being Zr a ductile material, can be considered as a good candidate to accommodate the residual stresses of the W/steel joint, even if the author's results showed low joint strength. Finally, more investigations need to be done in order to understand if, optimizing the HIP parameters, it can be used as interlayer material in fusion applications.

For HIP joining of W/Steel, Jiajia Zhang et al. [32] used an interlayer of copper. In particular, they varied the holding time of the HIP process from 0.5 to 2 h in such a way to observe the changes in the microstructure of the joint. The other parameters were: $T_{HIP}=1050^{\circ}\text{C}$, pressure=150 MPa [32]. As result they obtained samples free of defects or unbounded regions, because the copper presents a good wettability with both materials (W and steel). Moreover, no brittle intermetallic compounds were found at the W/Cu and Cu/steel interfaces. This can be the reason for which no brittle fractures were observed and instead a plastic surface fracture was noted in all the samples, as fig. 10 shows.

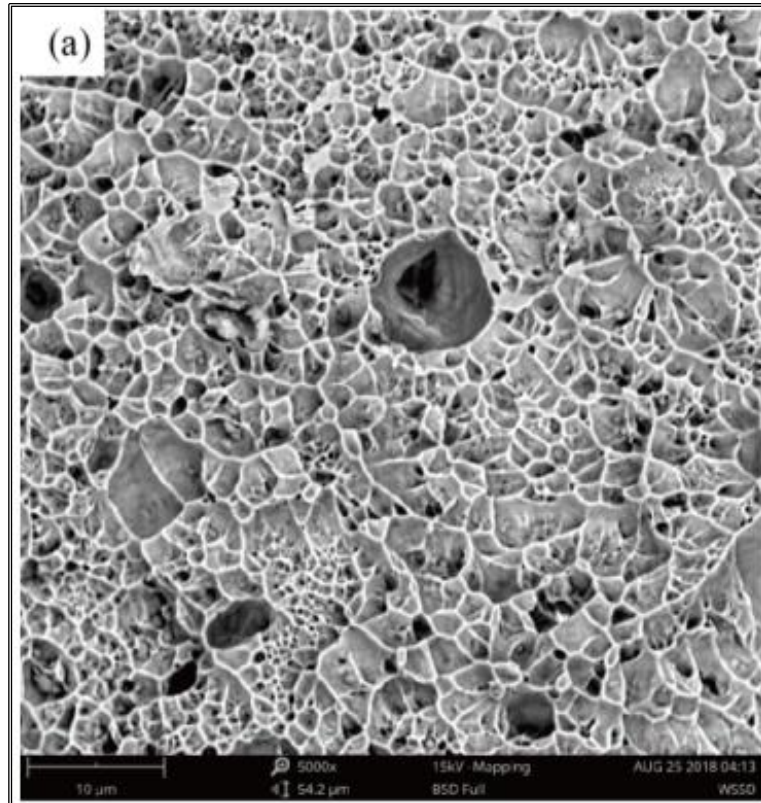


Figure 10: Example of plastic fracture of SS316L surface [32] after 2 h of HIP and tensile test

The authors noticed that with increasing holding time up to 2h, the strength of the joint increased, finding as maximum value for the tensile strength 480 MPa [32], higher with respect to other types of materials. It is noticeable that with post heat treatment the strength of the joint decreases, but it is also important to highlight the fact the copper constitutes an important material for W/steel joints because it has a significant capability to sustain the thermo-mechanical residual stresses.

Ni was used too as interlayer material, in order to promote the wettability, after the HIP process, between interlayer and base materials.

Yue Wang et al [33], experimented a W/Ni/steel joint, varying the thickness of the interlayer, in order to understand the behavior of the joint and the influence of the thickness of Ni on it. They performed the hot isostatic pressing diffusion bonding at 1020°C, with a pressure of 130 MPa for 5 hours [33].

The authors demonstrated the dependence of the microstructure, the Post Welding Heat Treatment (PWHT), and the strength with respect to the interlayer thickness. In particular, they noticed that the uniformity of the interface joint changed according to the interlayer. For thickness up to 30 μm, the presence of voids and cracks caused a reduction of the joint strength, affected also by the formation of a brittle reaction layer.

When Ni substrate is increased up to 50 μm the compactness of the seam region increased, and the post welding heat treatment can be considered beneficial because it improves a diffusion layer between the materials, thing that with higher values of thickness is not true. In addition, from the joint strength point of view, they discovered that the tensile strength of the joint did not have a constant growth: only when the thickness increased from 50 μm to 80 μm (with PWHT) the shear strength had a significant evolution.

Besides, they found that if the W side is also polished, and so the roughness of the substrate is decreased, the joining is improved, thanks to the fact that the two bonding faces are closely in contact. However, a good metallurgical and mechanical bonding was achieved [33]. The following figures show the dependences of the parameters previously described, with and without Ni interlayer.

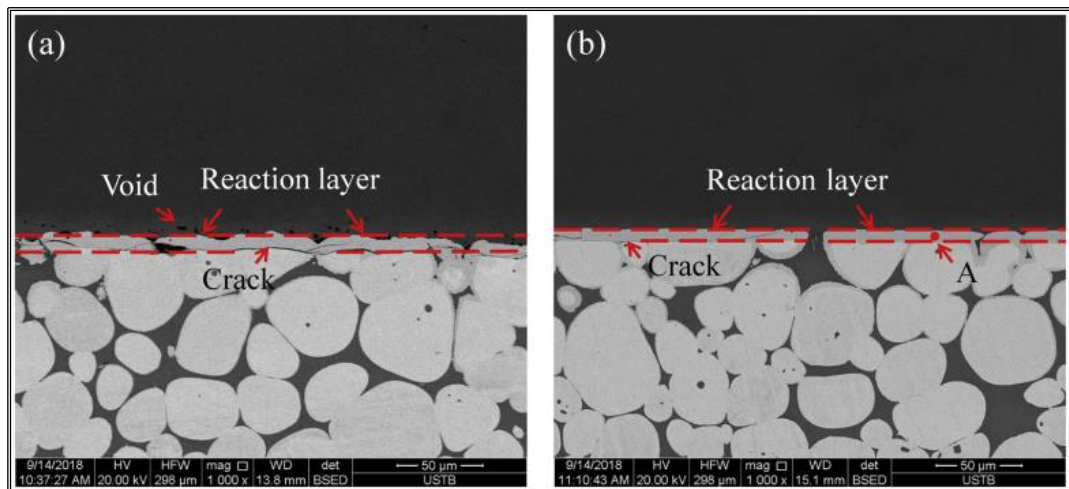


Figure 11: Microstructures of the W/steel joint without interlayer: a) sandblasted, and b) polished [33]

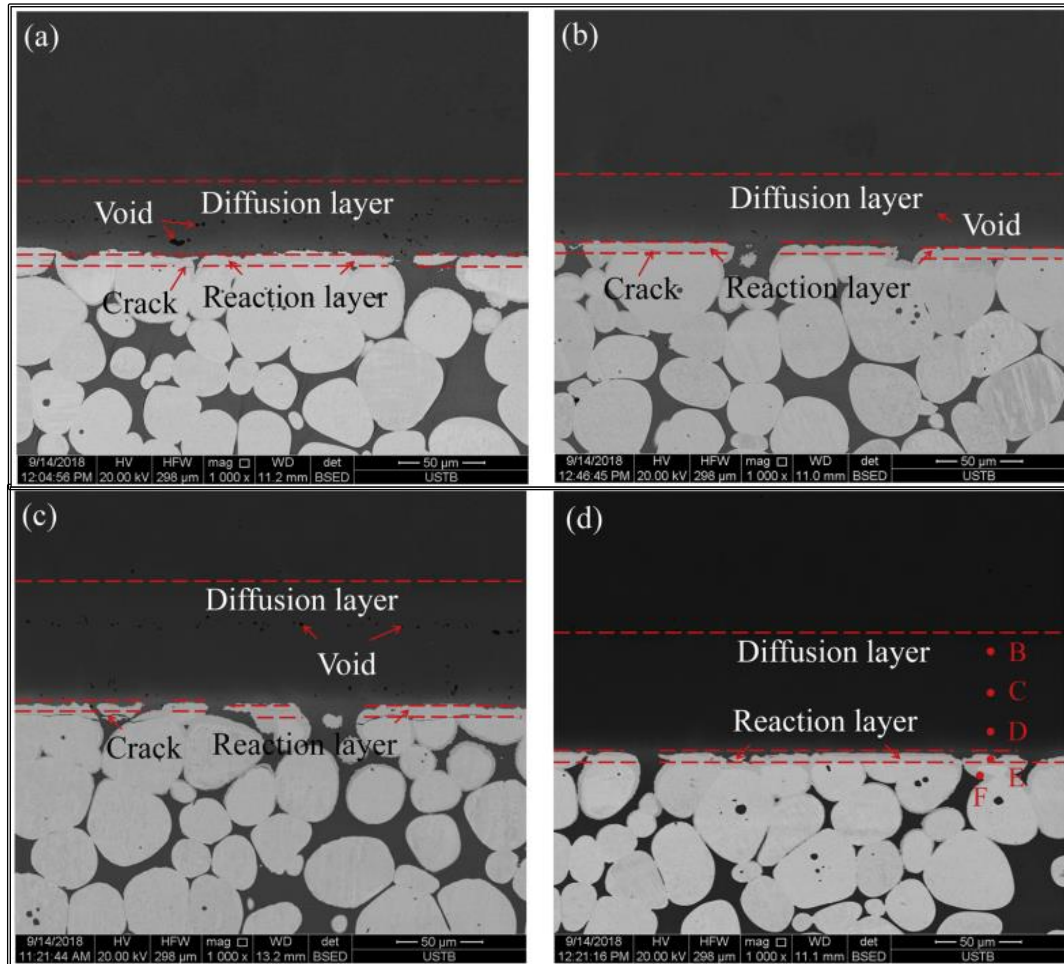


Figure 12: Microstructures of the W/steel joint with Ni interlayer: a) sandblasted-30 μm , b) polished-30 μm , c) sandblasted 50 μm , d) polished-50 μm [33]

One of the most recent research concerning the W/steel joints with HIP is the one of E. Sal et al. [34]. They used a self-passivating type of W (10Cr-0.5Y (in wt.)) that, with respect to the pure one, is capable to create a protective layer in case of Loss Of Coolant Accident (LOCA) preventing the failure of the system due to the formation of volatile compounds.

In particular, they performed the HIP in two ways, with different parameters, in order to compare the samples with and without the post heat treatment. The first approach was carried out at 700°C, with 100 MPa as pressure for 1 h. The second one was at 980°C, with 140 MPa for 3 h [34].

The resulting joints appeared without any cracks or pores at low magnification (see fig. 13), and at higher magnification an oxide layer with some particles is visible. From the analyses, there are Fe-rich compounds inside the Cu band, and in the Cu/steel region more defects and oxides were detected.

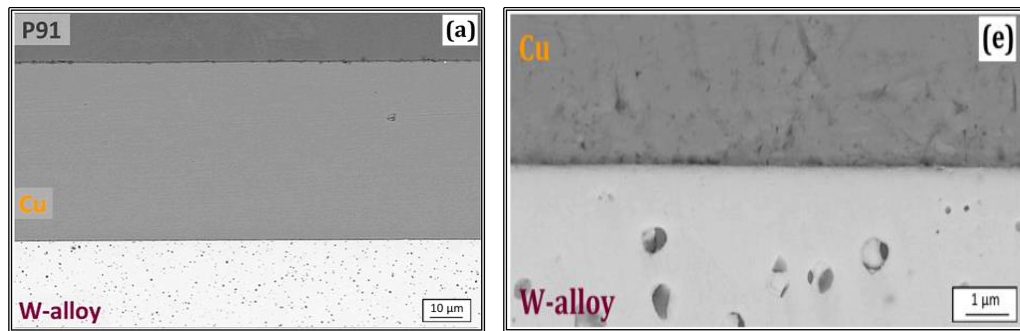


Figure 13: SEM magnifications of the joint with the first HIP (700°C) [34]

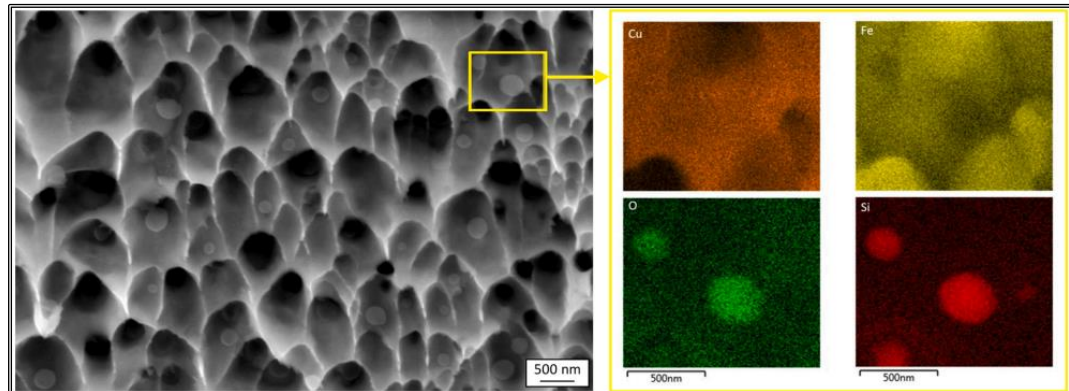


Figure 14: fracture surface at the steel/Cu side of the joint (980°C) with the presence of Si-oxide [34]

It was found that residual oxygen present at the Cu/steel interface influenced the formation of oxides in that region. In fact, from fig.14 it is possible to observe Si-oxide particles inside the dimples, produced by the oxygen diffusion into the steel. To avoid their production, a Cu interlayer free of oxygen may be used.

As concern the mechanical properties, the shear strength of the samples was different, according to the parameters of the HIP and the consequent heat treatment to recover the steel properties (see fig.15).

When the temperature is low, the shear strength is low. When the temperature is increased (980 °C) there is a significant growth of the shear strength of the joint, leading to a very good result. Nevertheless, it is noticeable that with high temperatures a tempering heat treatment for the steel is necessary which leads to a reduction of the strength, as the following graph shows.

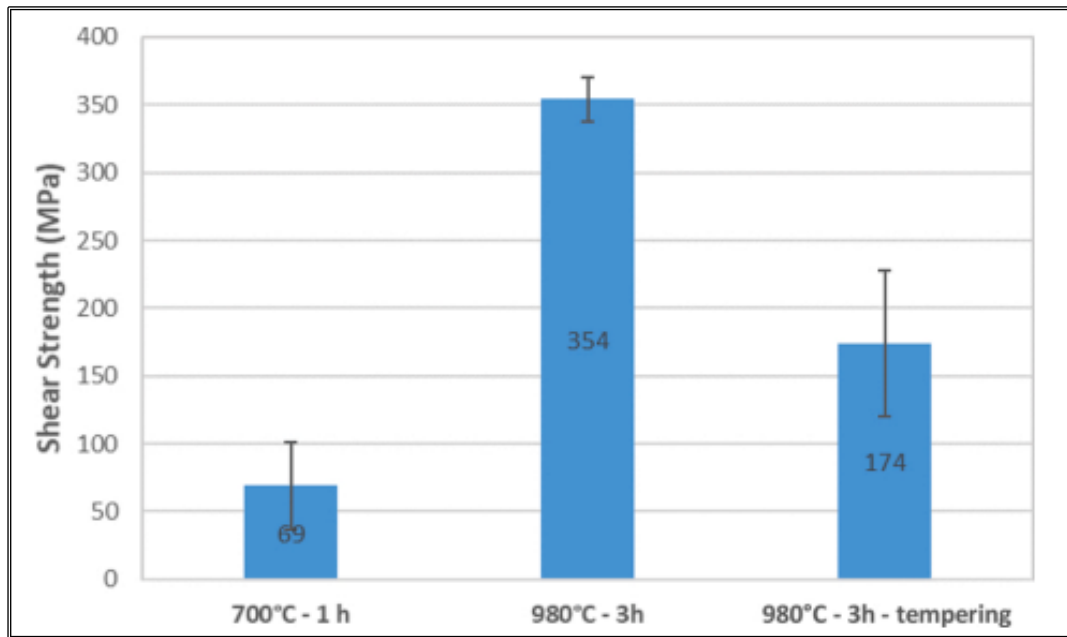


Figure 15: Shear strength of the joints trends according to the type of HIP [34]

In general, the HIP technology represents a valid solution to produce W/steel joint, because according to the previous data, it provided very good results. Besides, the high pressures allow to manufacture joints with a high density, reducing the pores inside the material that appears more homogeneous. However, this process involves high temperatures and pressures that may lead to elevated costs of manufacture and production. For this reasons, further investigations are needed to find the optimal parameters in terms of costs and time.

2.3 Functionally Graded Materials

In order to smoothly distribute the stresses at the tungsten/steel joint interface, Functionally Graded Materials (FGMs) are arousing interest in the nuclear material field.

The presence of interlayers with varying properties can reduce the thermal-induced stresses and strain in the joint region.

Different technologies have been developed for FGM fabrication as uniaxial hot pressing [35], laser cladding [35], atmospheric plasma spraying [35], spark plasma sintering [35], and Field Assisted Sintering Techniques (FAST) [36].

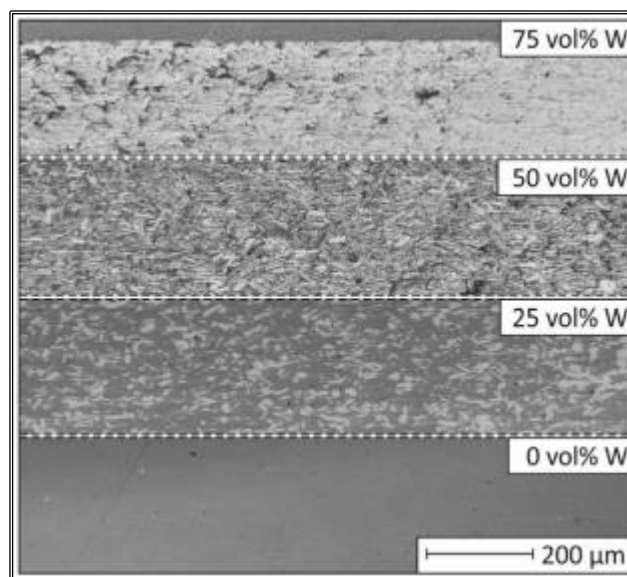


Figure 16: Example of a FGM Fe/W composites [37]

S.Heuer et al. [36] developed two different types of coatings deposited on steel substrates: one uniform with a constant ratio between the tungsten and the steel, and the second with FGMs.

They preheat the substrate at different temperatures (500 °C, 700°C and 900 °C) so as to analyze the responses of the material in function of the temperature.

The tungsten volume fraction was: 0, 25, 50, 75, and 100. Firstly, they noticed that the microstructure of both types of coatings was almost similar and four different components were present as it can be seen from the figure 17.

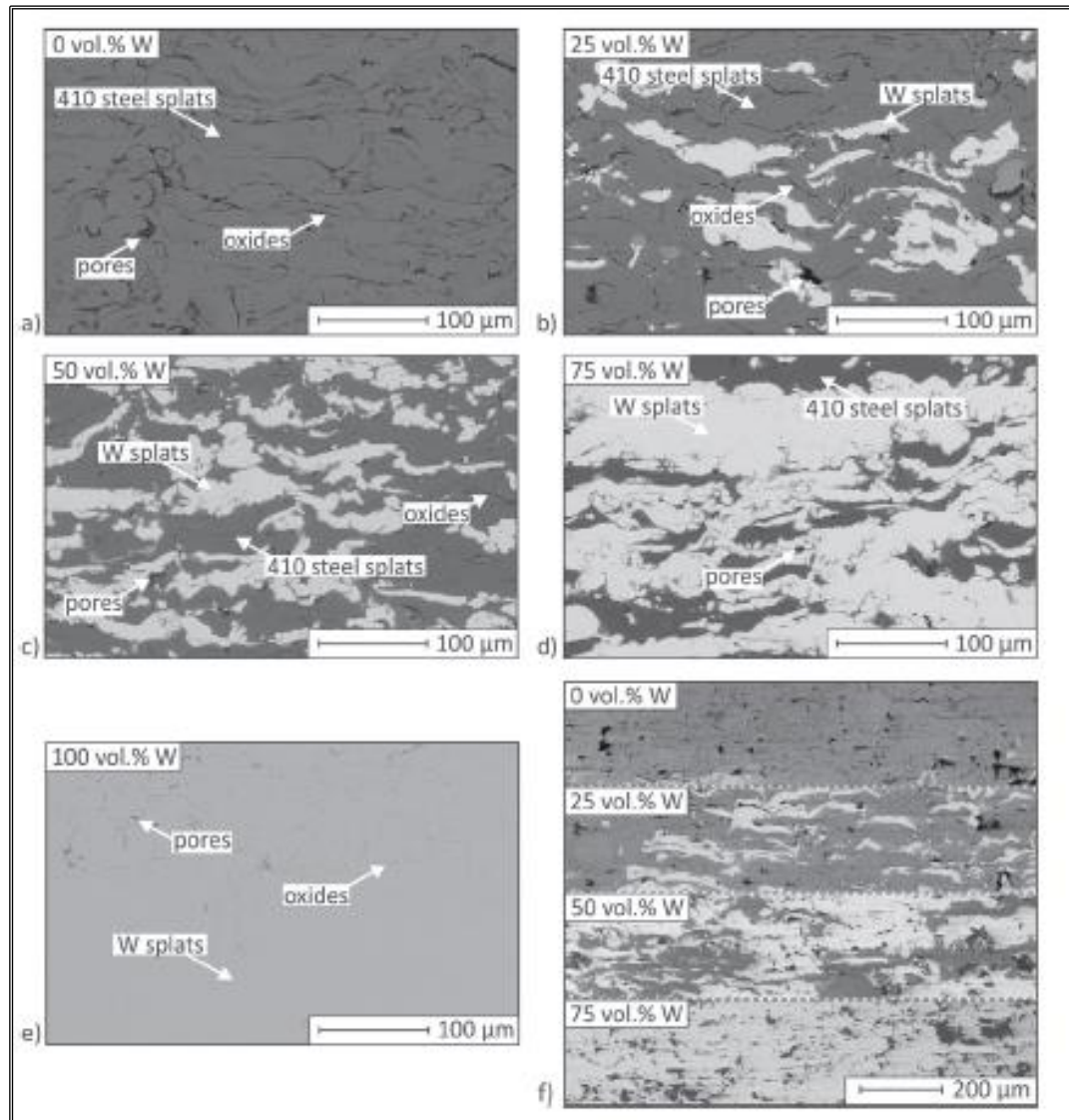


Figure 17: Cross-sections of uniform coatings and steel/W FGMs at different W vol. fractions: a) 0 %, b) 25 %, c) 50 %, d) 75%, e) 100%, f) FGM [36].

Both porosity and oxide concentration were not influenced by the preheating of the substrates, but they found that the latter was dependent on the content of W in the layer, and it is also responsible for the ductility of the material. For these reasons, it is necessary to reduce as much as possible the content of oxygen.

Besides, they discovered that above the temperature of 700°C for the substrate preheating, a certain amount of intermetallic precipitates arose. This means that the favorable maximum temperature for preheating is 700 °C. As far as the intermetallic phase and precipitates are concerned, a set of heat treatments in sintered Fe/W composites was

carried out in [37], in order to understand the dependences between ageing and the formation of other constituents. It was found that the hardness of Fe_7W_6 is three times higher than the ones of the tungsten.

For this reason, it is reasonable to say that the interface between the tungsten and a reaction layer full of Fe_7W_6 compounds represents the weakest part of the joint, because brittle intermetallics may lead to a premature failure of the bond.

Finally, new experiments are necessary to better understand the changes of Fe/W composite at the microstructure scale.

From a thermo-mechanical point of view, according to studies reported in [38] ideally the number of FG interlayers can be considered 10 [38].

S.Heuer et al. [38] made some experiments in which they compared two models: one with a 1 mm thick FGM, and the other representing a direct joint between tungsten and EUROFER. Besides, they varied the number of FG interlayers from 100 to 1, and the relative thickness from 0.3 mm to 3 mm.

They found that the optimum for the number of interlayers was three because in this way the deformations are limited and minimised, and a good value for the width varies according to the heat load: for 4 MW m^{-2} it can be of maximum 16 mm, and for lower heat loads the width must not exceed 20 mm.

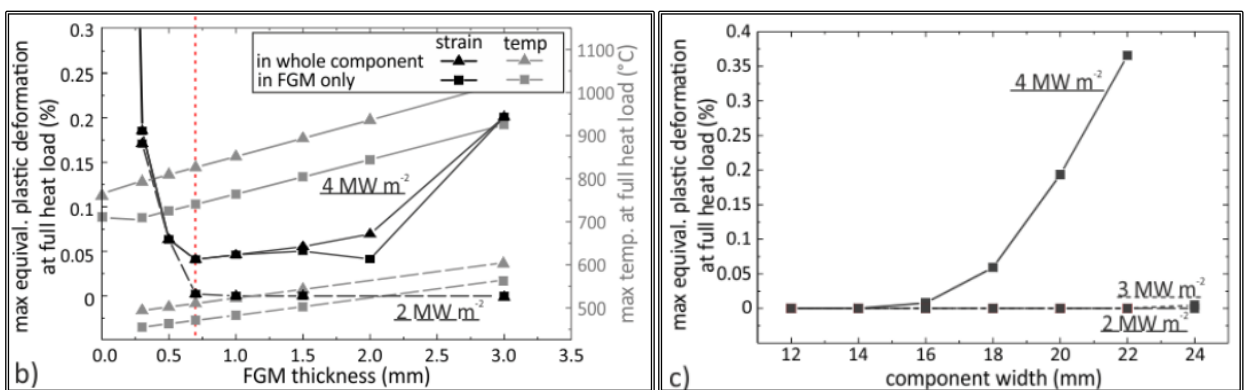


Figure 18: Trend of the FGMs thickness and width in relation to the plastic deformation [38]

Finally, for the FGMs thickness, it was found that 1 mm is good for heat loads up to 3 MW m^{-2} , but it can vary from 0.7 mm to 1.5 mm [38].

It is significant to highlight that the use of FGMs for the tungsten/steel joints, can reduce of 600 times the macroscopic plastic deformation, so that to smooth the stress-strain peaks at the interface. The continuous development of these kinds of substrates may lead to a very important technology able to withstand at the aggressive nuclear conditions.

2.4 Brazed joints

ITER, and subsequently DEMO, requirements need for a technology that must ensure reliability and availability. The continuous investigation on tungsten/steel joints is leading the scientific community to converge on a solution, for the short time, that is based on the brazed joints. As said before, the brazing joining technology presents some advantages that make it suitable for the assemblies of ITER divertor and first wall.

This method has been developed in different ways because according to the type of filler material, and to the brazing condition the response of the joint is not always the same. For this reason, the brazing method is carried out using filler materials fabricated in different ways and forms.

2.4.1 Brazing with powders

J.Prado et al. [39] used as brazing material a mixture of titanium and iron powders (86Fe-Ti) in order to create tapes as filler. They perform the brazing procedure at 1350 °C for 10 minutes with a heating and cooling rate of 5 °C/min. As result, the experimental studies showed the formation of a continuous layer near the interface area, the presence of Fe₂Ti, and TiC phase which create a not homogeneous microstructure of the joint. Therefore, the inter-diffusion of Ti, C, and Fe in the substrate of tungsten caused an interface displacement of 25 μm [39].

Having regards of these results, a new system was developed in the brazing field with powders, related to the use of fillers based on copper. The same authors in [40] used a mixture of titanium and copper pure powders fabricated as Cu-20Ti. The brazing was carried out in a high vacuum furnace, and the conditions were: 690°C as brazing temperature, a dwell time of 10 minutes, heating and cooling rates equal to 5°C/min, with a residual pressure of 10⁻⁶ mbar. The microstructure was constituted in majority by a copper

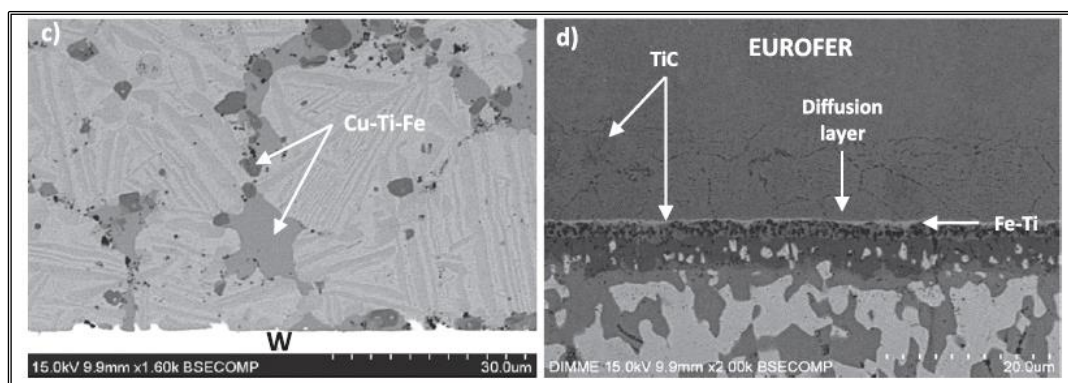


Figure 19: Overview of tungsten and EUROFER interfaces [40]

matrix, but they also detected the presence of intermetallic phases, as Cu_4Ti , and TiC . The precipitation of the latter inside the copper matrix was concentrated in the region of the diffusion layer.

In order to improve the resulting joints, they experimented a new type of powder-based filler material, changing the ratio between the copper and titanium [41]. 80Cu-Ti filler was produced with pure and alloyed powders, to demonstrate the fact that the use of a mixture of alloyed powders, with respect to a pure one, could represent an advantage. The use of alloyed powders, in fact, can reduce the heating stage of the brazing procedure of three times. Two different conditions were analyzed in which they modified first the dwell time, maintaining the same brazing temperature (960°C), and secondly, they reduced the brazing temperature conserving the dwell time. Also in this case, the microstructures were mainly constituted by a copper matrix in which Cu_4Ti phases and ternary compounds of Cu-Fe-Ti were present.

In general, it is reasonable to say that no detachments or discontinuities were found at the interface. The wettability of these filler materials is good so as to avoid any kind of wetting problem. In both the joints with Cu-based fillers, it was found a reduction of hardness in proximity of the seam region, in particular at the EUROFER side, probably caused by diffusion phenomena inside the steel.

Liangxing Peng et al. [42] used Cu-22TiH_2 as filler material obtained by mixing the copper with TiH_2 powders. Computing the brazing at 1173 K for 10 min, they demonstrated that the use of the brazing material was a good choice due to the fact that no cracks and discontinuities were revealed and the shear strength (98 ± 21 MPa) was promising. Also here, compounds of Ti and Fe, reaction layers, and recrystallization phenomena changed the hardness on the steel side of the joint.

Nevertheless, the scientific community is working on this, trying to change the brazing parameters, in order to find the optimum for the joints.

2.4.2 Brazing with liquid-forming interlayers and electroplating

It is worth to consider some studies on joints with liquid-forming interlayers and electroplating. Wen Zhu et al. [43], made brazing with lower temperature (1090°C for 5 minutes) with respect to the case in which Fe-based filler materials are used. They applied a coating assembly of Ti-fe-Sn made by electroplating to make a joint of tungsten and CLF-1, a Reduced-Activation Ferritic-Martensitic steel (RAFM) [43]. It was found that

according to the concentration/thickness of Sn, the joint presents a favorable condition in which high strength and stability during thermos-cycling can be reach.

Wolfgang Krauss et al. [44] experimented W/steel joints with Ni-Cu base filler and Pd-Cu-based filler. The brazing was done with a temperature of 1100 °C for 10 minutes. In both cases a good bonding was reached thanks to the electroplating of the base materials, even if some reaction compounds occurred. No evident cracks or wetting problem were found and it was proved that both Ni and Pd present very good properties in activation for brazing. Nevertheless, Ni must be subject to control according to its concentration for neutrons, so it is possible to replace it with Pd for brazing with Cu.

For divertor components applications, Qingshan Cai et al. [45] investigated Ti-Ni liquid-forming interlayers. The brazing process was performed at 1050°C for 1 hour with different heating and cooling rates (20°C/min and 5°C/min respectively). The observed joint was constituted in the following way: W/Ti/Ni/Ti/steel.

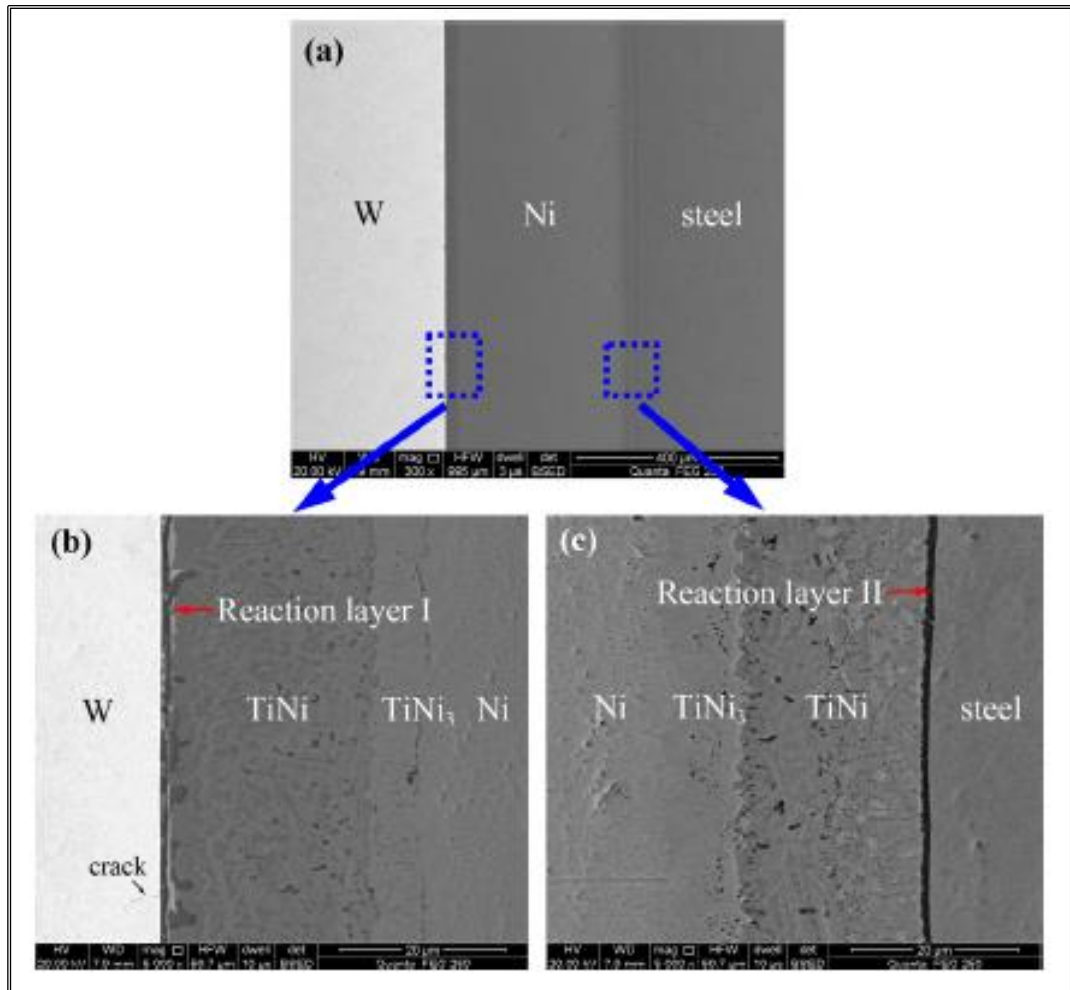


Figure 20: W/Ni and Ni/steel SEM magnifications [45]

It is possible to observe from the figure 20 that no significant discontinuities were present in the interface regions and the joint was essentially free of significant cracks.

However, the presence of intermetallics and reaction layers made the joint not so reliable. It can be said that also here the presence of TiC phase at the Ni/steel part makes it the weakest part of the joint, characterised by a typical brittle fracture. Even if the titanium is considered a very good element to improve wettability at the joint interface, it forms a lot of compounds, especially TiC, that fill a reaction layer and make the seam the weakest part of the joint.

It is reasonable to say that the EUROFER interface is one of the most problematic part of the joint and during brazing it is subjected to different phenomena as inter-diffusion of elements by the filler and consequent softening in the seam area. For these reasons, scientists developed W/steel joint using ODS-steel as base material.

In [46] B.A.Kalin et al., brazed a W/ODS-EUROFER steel joint using as filler materials alloys based on Ti and Fe, at 1150°C, using a Ta spacer to reduce and smooth the residual thermal- stresses. The resulting joints showed continuity in the joint region and good stability for thermocycle process. Naoko Oono et al. [47], joined the ODS ferritic steel K1

(Fe-19Cr-0.3W-0.3Ti-0.3Y₂O₃) with tungsten, using as filler material an amorphous alloy based on iron (Fe-3B-5Si). Also here there were no problem of wetting, but the analyses showed that the diffusion of Si and W into the ODS steel was deep, and depends on the temperature of brazing. Besides, they found a high concentration of Cr, C, and W into the layers causing a reduction on mechanical properties of the joint, in particular the strength. It is also important to highlight the fact that Fe and Cr did not penetrate inside the ODS steel, so it is necessary to have more investigations in order to reduce the diffusion of elements into the steel material of the joint.

2.4.3 Brazing with interlayers and foils

Considering the mismatch between the coefficients of thermal expansions of the base materials, the brazing technique showed better results with the use of foils/interlayers as fillers. In fact, thanks to the more homogeneous surface of bonding, there is high capillarity at the interface. Nickel-based filler metals have been tested due to their good properties for corrosion and high temperature service performance. T. Chehtov et al. [48], investigated W/steel brazed joints using two kinds of high temperature filler materials based on nickel: STEMET 1309 (Ni, Cr 15.0; Si 7.5; Fe 4.0; Mo 4.0; B 1.5) and the commercial paste BrazeTec 1135 (Ni; Cr 19.0; Si 10.1; B 0.003; C 0.06; P 0.02). The resulting joints demonstrated that the braze region was the weakest because of the residual stresses and low strength. Even though the brittle behavior and the strength of the joint increased with increasing temperature, the mechanical properties after 1000 °C changed and the residual

stresses in the brazed zone were higher than strength.

Yunzhu Ma et al. [49], experimented a joint between a high Cr ferritic stainless steel and tungsten, by using a Ni-base alloy (Ni-7Cr-5Si-3B-3Fe in wt.%) as brazing material. In order to minimise the residual stresses after brazing, a 0.3 mm thick slice of Vanadium was used because it presents a coefficient of thermal expansion with a value in the middle between the tungsten and the steel ($\alpha_V=8.3 \times 10^{-6} \text{ K}^{-1}$) [49]. The results showed a well

bonded joint, without any relevant cracks or pores. The tensile strength of the joint was about 143 MPa. However, it is important to highlight the fact that a vanadium boride layer was formed at the seam region and, together with some brittle intermetallic compounds, caused a typical brittle fracture, as fig.21 shows.

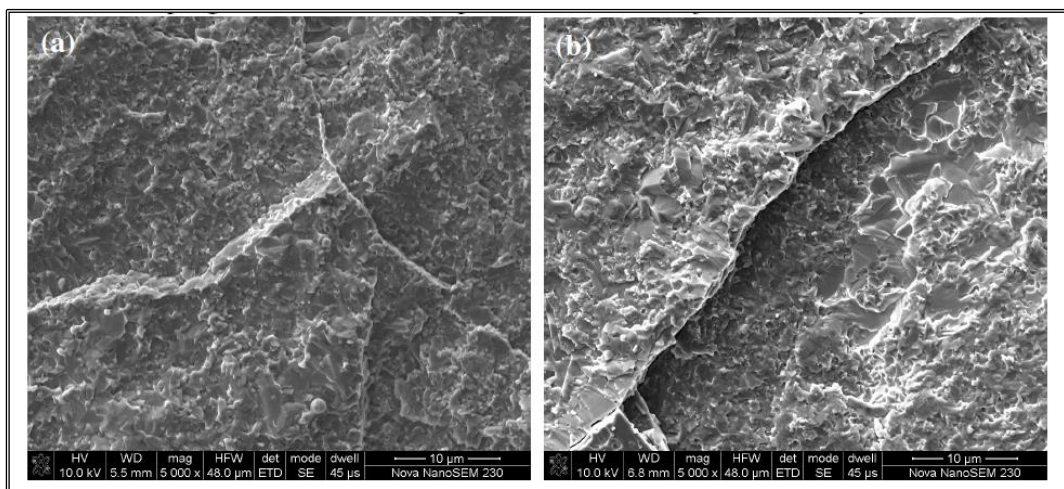


Figure 21: Brittle fracture at a) tungsten side, b) steel side [49]

The seam area, presenting a hardness of 25 GPa, constituted the weakest part of the bond.

Regarding the mechanical properties of the joint, Zixuan Wang et al. [50] tested a brazed joint of W (99,95 % purity) and high Cr ferritic stainless steel, with a Ni-based alloy as brazing filler (Ni-7Cr-5Si-3B, in wt.%), in which they changed the interlayer material from Vanadium to Niobium. In particular, they used a 0.1 mm thick intermediate Nb ($\alpha_{Nb}=7.07 \times 10^{-6} \text{ K}^{-1}$), to accommodate the residual stresses from brazing.

The analyses revealed a good bonding between the brazing filler and the base materials, and only in the W/Nb interface few microcracks. The existence of compounds boron-enriched and W-Ni type at the diffusion zone, made the latter the most hard (23 GPa) and weak region of the joint, causing a decrease in mechanical properties. Moreover, mechanical tests showed two types of brittle fracture, distinguishable in figure 22, in which it is possible to observe different regions, according to the element compounds present.

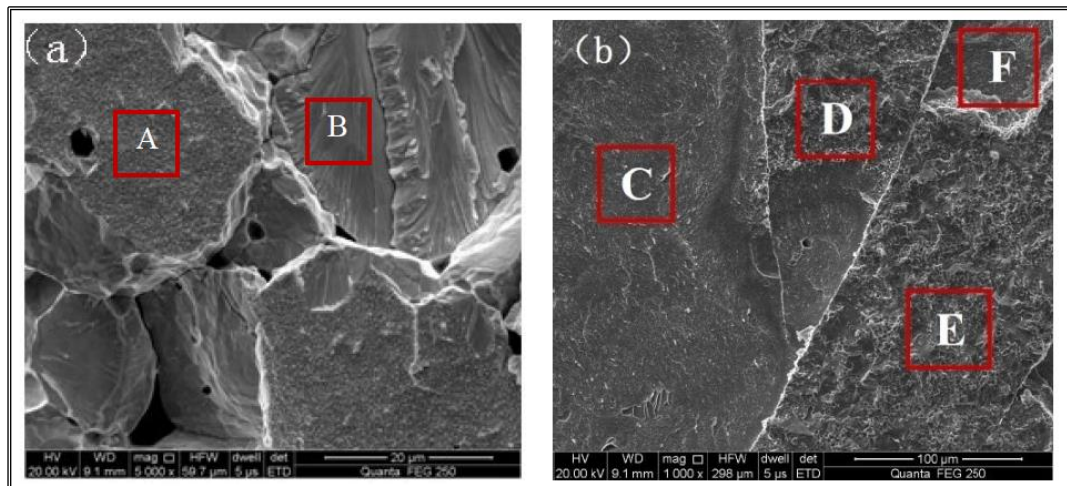


Figure 22: SEM images of the two fracture modes [50]

Nevertheless, this result represents a step forward for brazing technique because the strength joint was higher than the previous one of about 141 MPa (284 MPa) and the presence of the niobium interlayer decrease the residual stresses.

Further investigations with vanadium as interlayer were done by Bachurina et al. [51], in which two types of joints were developed. They used as base materials tungsten and the ferritic-martensitic steel RUSFER EK-181, and as brazing fillers two Cu-Ti based alloys: STEMET™ 1203 (Cu-50Ti) and STEMET™ 1204 (Cu-28 Ti) creating : EK-181/Cu-28Ti/V/Cu-50Ti/W and EK-181/Cu-50Ti/V/Cu-50Ti/W [51]. Also two different brazing conditions were used to fabricate the joints, both having the same brazing temperature equal 1100 °C. In order to test the reliability of the samples, thermocycling tests were conducted and each specimen was heated (up to 700°C) and quenched for 30 and 50 cycles. The strength before and after the thermocycling tests were: 205 ± 12 MPa and 126 ± 40 MPa for Cu-28Ti, 98 ± 12 MPa and 30 ± 12 MPa [51]. According to these results, the Cu-28Ti alloy was chosen for the traditional brazing and the successive investigations on the

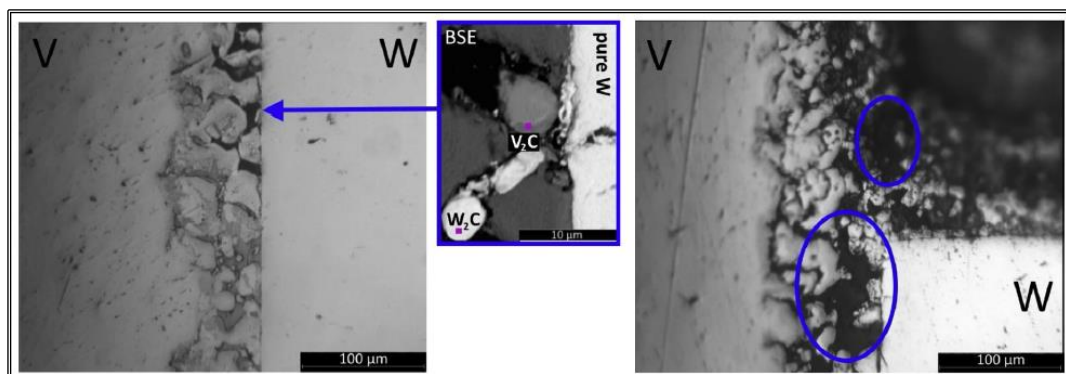


Figure 23: V/Cu-50Ti/W seam with magnification of the compounds and filler zone with defects [51]

joints showed the formation TiC , V_2C , and W_2C phases, which are responsible for the weakening of the bond, and the consequent presence of defects.

However, the joints made with Cu-50Ti showed a thicker carbide layer which involves a decreasing diffusion of iron from the steel that can be considered as a good point, but also a reduction of the joint strength due to the compensating formed layer which decreases the capability, at the interface, of lessening the residual thermal stresses.

These outcomes demonstrated that the use of Cu-28Ti alloy filler is preferable to Cu-50Ti and, from the point of view of strength, to a Cu-Ge-based filler material in which a degradation of the microstructure occurred after 50 thermocycles [52].

The latter comparison can be justified by the fact that in Cu-28Ti joint the lower presence of Cu reduces the diffusion of its precipitates into the steel grain boundaries and also due to the strengthening operation of the formed carbides.

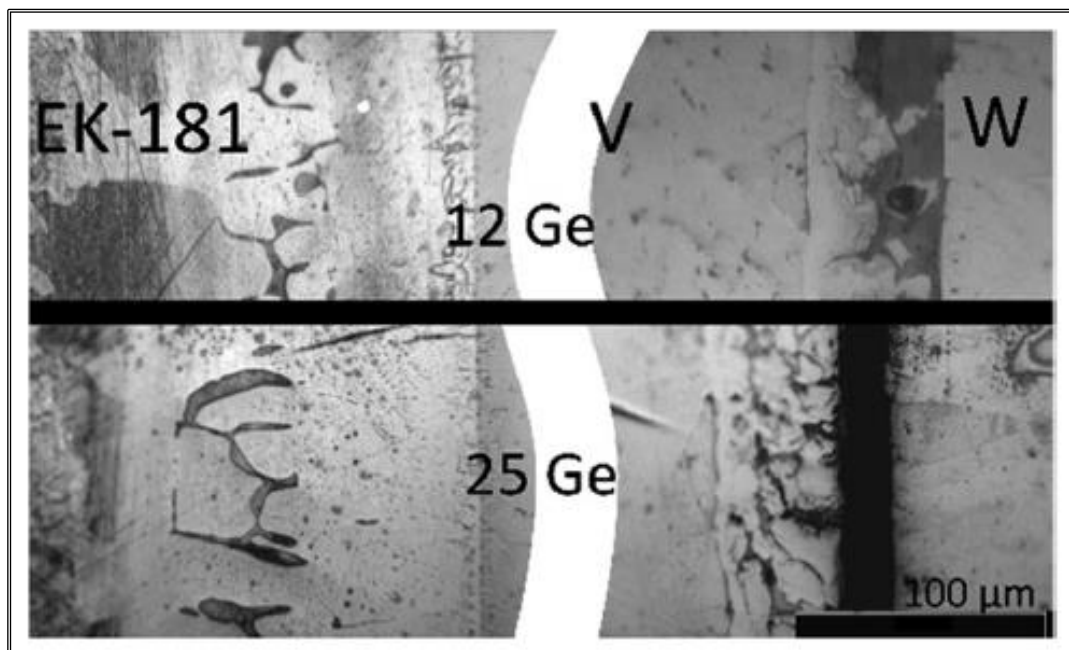


Figure 24: Cu-12Ge and Cu-25Ge after thermocycle process [52]

Nevertheless, these results led to a further investigation of W/steel joints using Vanadium as interlayer and brazing filler materials base on copper, titanium and germanium.

Bachurina et al. [53] kept to test the W/EK-181 joints comparing different samples containing vanadium and tantalum interlayers. The brazing material was again Cu-50Ti. As expected, the use of Ti led to a formation of carbides as TiCu, Ti₂Cu, and TiC phase, which imply a reduction of mechanical properties due to a softening area. In order to reduce the diffusion phenomena, a V interlayer and, after, a Ta interlayer were used. The latter did not produce big changes, but using a 200 μm thick interlayer of vanadium it was possible to reduce the residual stresses.

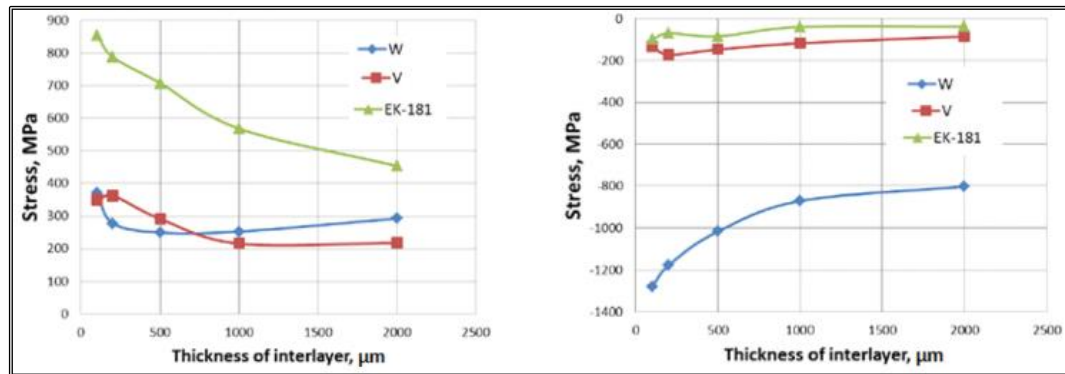


Figure 25: Compressive radial stresses and tensile radial stresses with a vanadium interlayer [53]

Besides, from figure 25 it is possible to observe that increasing the V thickness from 1000 μm to 2000 μm no big changes occur. However, in order to reduce the residual stresses at the interface region, an interlayer of V-4Ti-4Cr was used, together with Cu-50Ti as filler material.

The results showed a significant reduction in stresses, but the presence of Ti in the interlayer material has increased the probability of carbides formation at the seam zone which may led to a reduction in mechanical properties.

For this reason, the authors decided to change the filler material, to decrease the content of Ti in the joint. They used low-activation Cu-Ge-based alloys considering the low activity of Ge (9.32×10^{-10}) [53]. The resulting joints demonstrated the fact that TiC phases were absent and consequently also softening phenomena.

Despite of this improvement, the diffusion of iron inside the V-based interlayer occurred, and large cracks were observed after thermocycling. Finally, the authors suggested to add some alloyed elements to the Cu-Ge filler material, to try to stop the diffusion of iron at the interface.

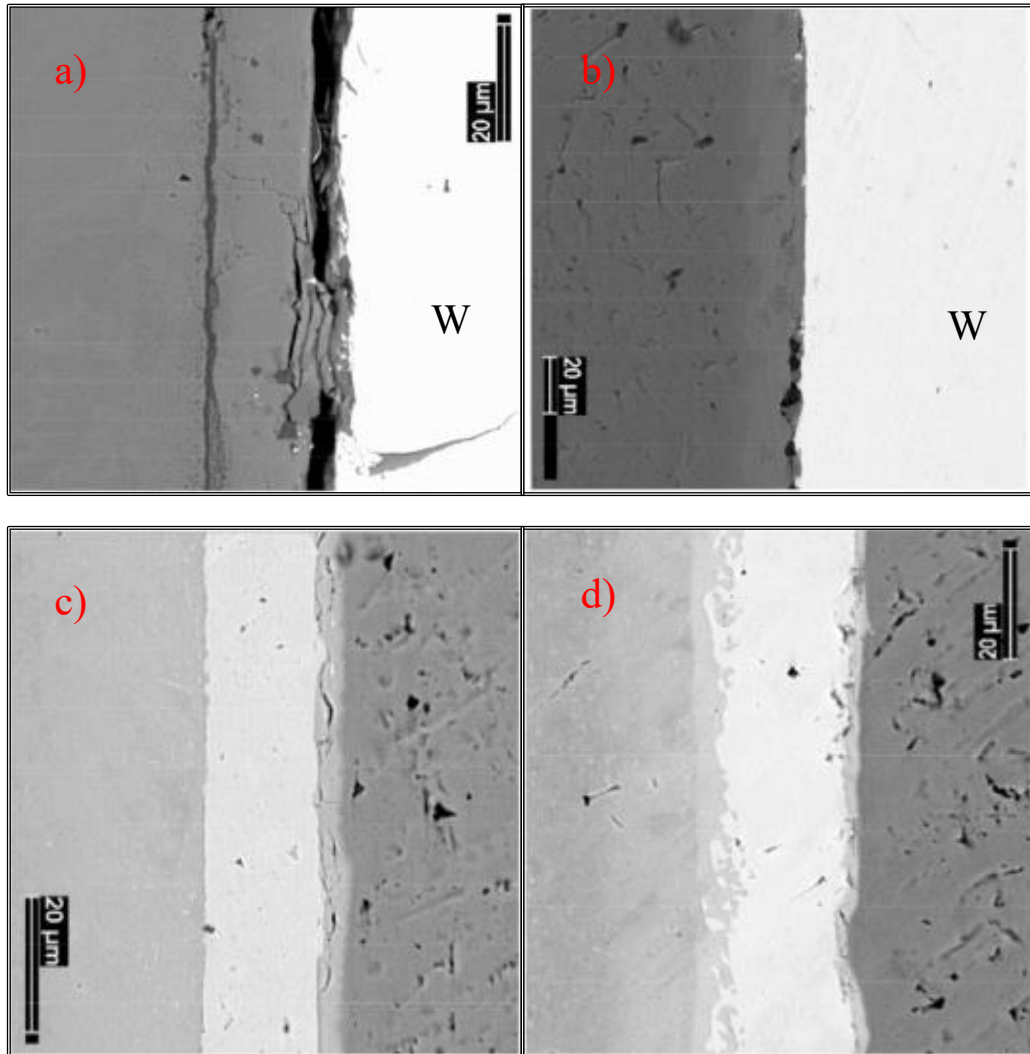


Figure 26: Microstructures after thermocycling of A) EK-181/W joint (Cu-50Ti filler), B) W/V-4Ti-4Cr joint (Cu-50Ti filler), C) EK-181/V-4Ti-4Cr joint (Cu-12 Ge filler), D) EK-181/V-4Ti-4Cr joint (Cu-25Ge filler) [53]

It has been established that vanadium represents a good material as interlayer to decrease the residual stresses at the joint interface. In fact, D. Bachurina et al. [54] developed different types of joints: EK-181 / Cu-12Sn / V / Cu-50Ti / W, EK-181 / Cu-12Sn-0,4P / V / Cu-50 Ti / W, and EK-181 / Cu-20 Sn / V / Cu-50 Ti / W [54].

Considering the samples, the tungsten was always brazed with Ti-based filler and the steel part with the Cu-Sn-based fillers with different concentrations.

Three different types of brazing conditions were applied, in order to analyze the behavior of materials with changed parameters.

The results highlighted a general decrease in strength of the joints after thermocycling tests and after the heat treatment in the steel. However, the resulting values of the shear strength were higher with respect to other kind of joints, and the maximum value was found in the sample with Cu-20 Sn as filler brazing material (160 MPa) [54].

As regards the use of interlayers, W. Liu et al. [55] investigated two types of W/steel joints placing in the middle a 0.5 mm thick Ta an Cu spacer, respectively.

The brazing filler used was a Ni-based alloy and the brazing process was executed at 1050 °C for 60 min. Both joints were fabricated with the Ni-base filler and the final results were good from a point of view of wettability and homogeneity of the interfaces. From the following figures the smoothed and clear seam region can be observed.

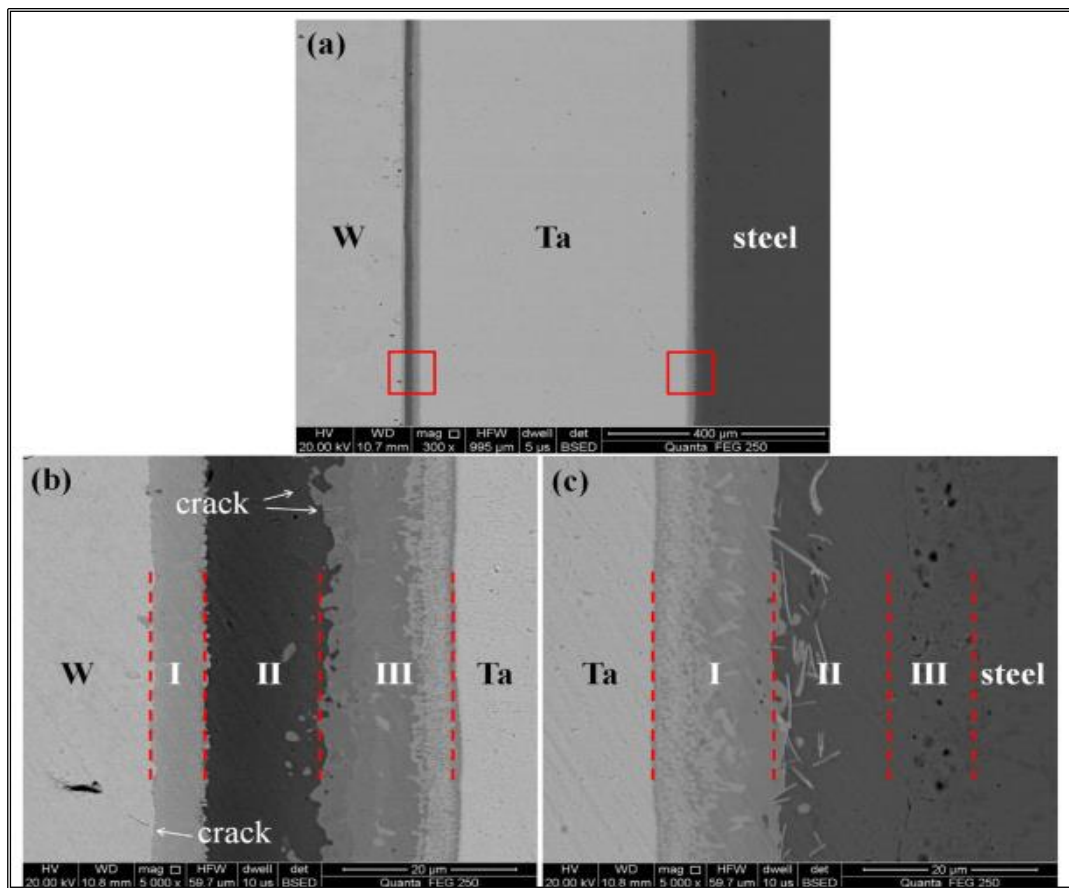


Figure 27: SEM general view of the W/Ta/steel joint with magnifications [55]

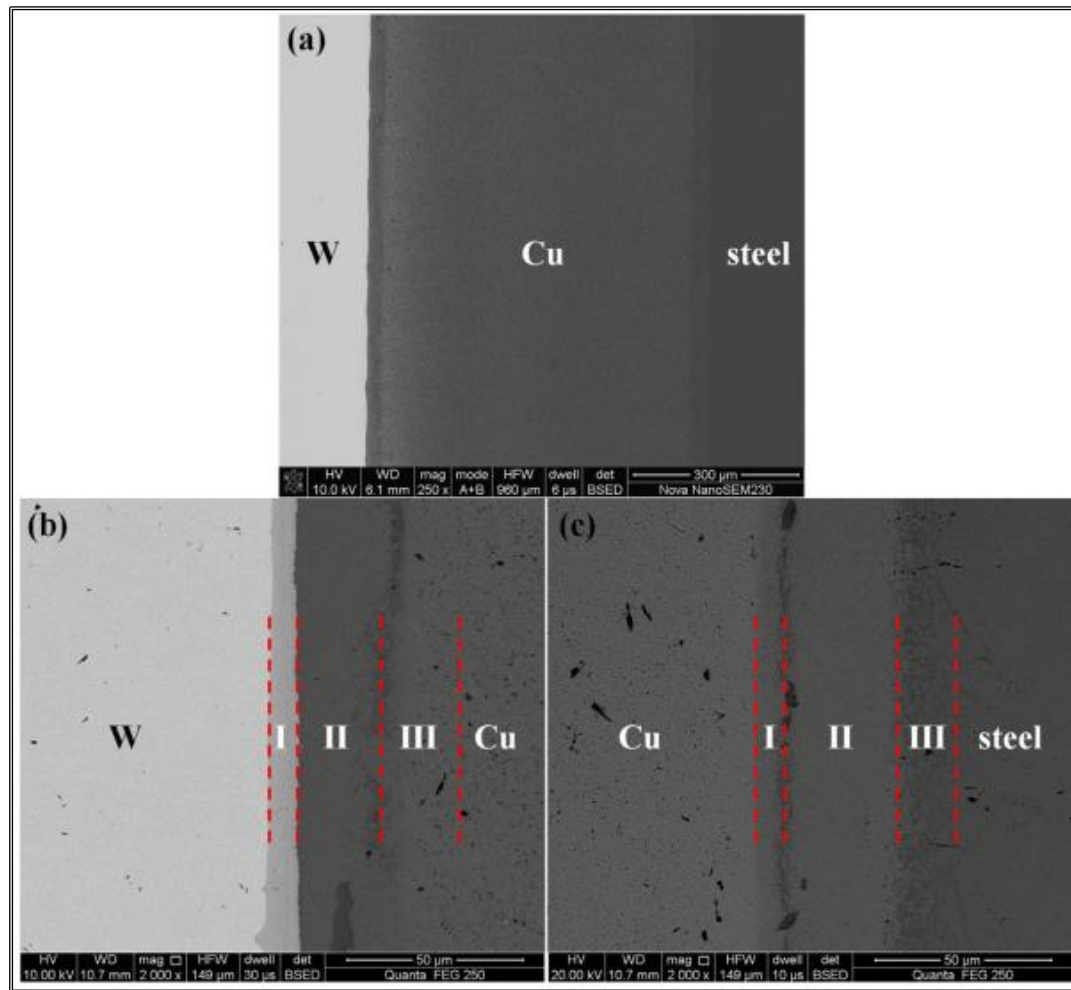


Figure 28: SEM general views of the W/Cu/steel joint [55]

Mechanical tests showed a typical brittle fracture for both samples, with the hard Ta interlayer and with the soft Cu spacer. The average strength of the W /steel joints was 257.8 MPa for the sample with Ta, and 276.7 MPa for W/Cu/steel [55].

These results demonstrate that a soft Cu interlayer in the middle of the W/steel joint can reduce the residual stresses and consequently improve the mechanical properties.

Following this concept, J. de Prado et al.[56] made some experiments considering the influence of the brazing temperature, thickness and Post Brazing Heat Treatment (PBHT) in the W/steel joints. In particular, they performed brazing using as filler material pure copper (>99,99%) strips of 50 and 250 μm respectively. The residual pressure was 10^{-6} mbar and the brazing temperatures were 1100°C and 1135°C, both for 10 min with a heating rate of 5°C/min.

In order to test different samples, some of them were subjected to PBHT at 760°C for 90 min, to recover the as-received properties of the steel base material.

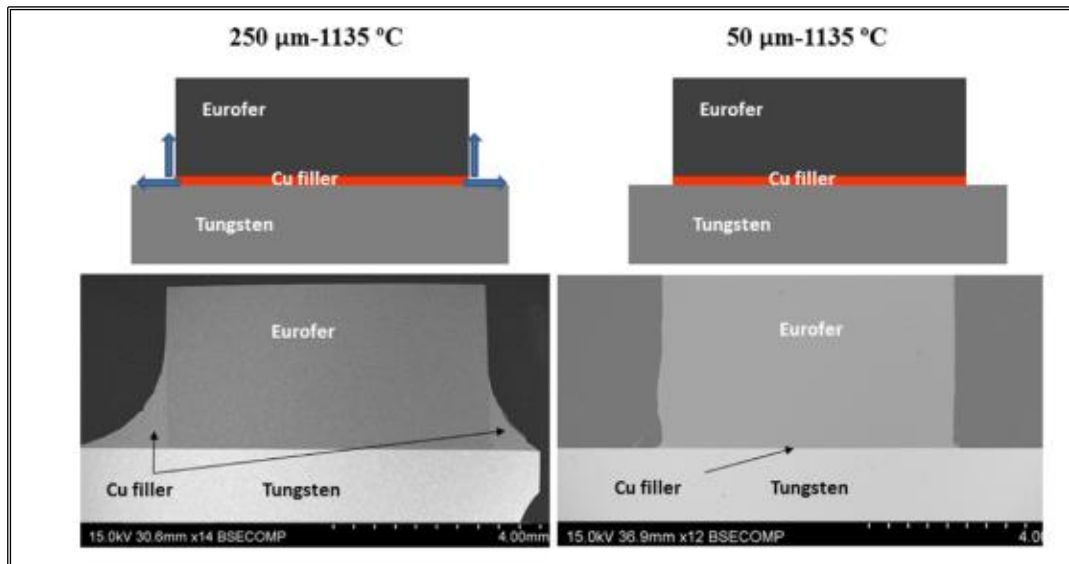


Figure 29: Schemes and SEM images of the exudation of copper in both brazing conditions [56]

From figure 29 it is possible to notice the exudation of copper after brazing, in particular in the case of Cu thickness equal to 250 μm because of the larger amount of filler. To this thickness is also associated the formation of a copper layer after brazing at 1135°C, because they demonstrated that at higher brazing temperature there is higher interaction between the brazing filler material and the base materials. More in details, with 50 μm of thickness, at lower temperatures, it can be seen that there is a lower content of copper after brazing, as the figure 30 shows.

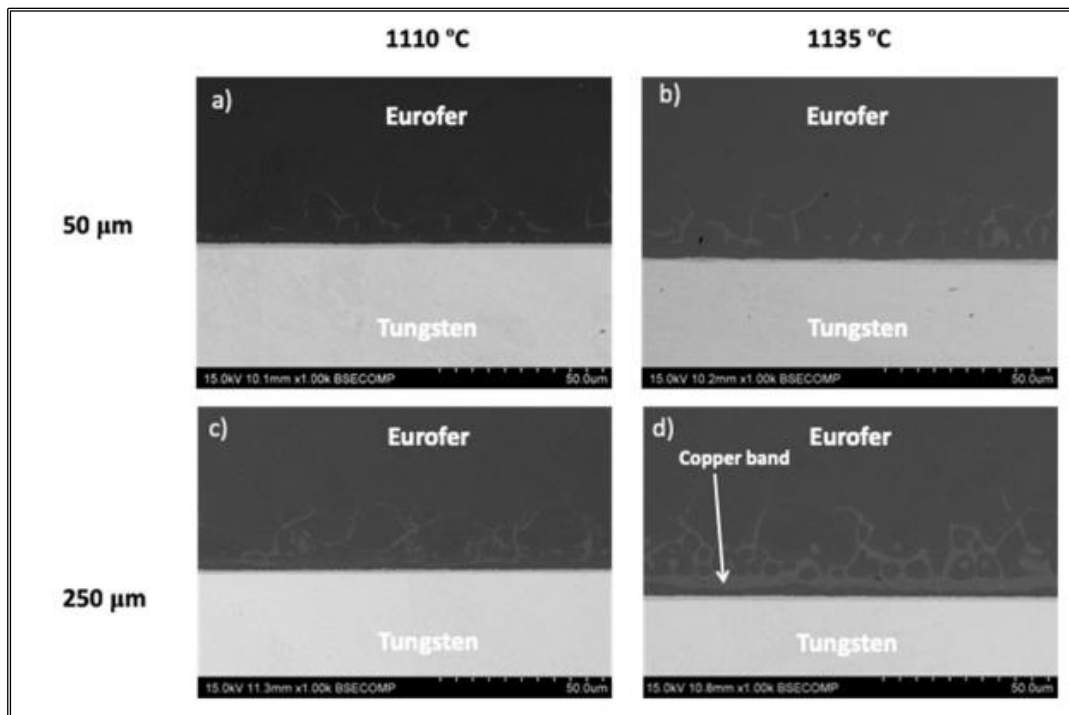


Figure 30: SEM images indicating the copper diffusion in the joint in a) 50 μm at 1100°C, b) 50 μm at 1135°C, c) 250 μm at 1100°C, d) 250 μm at 1135°C [56]

The authors demonstrated that the brazing temperature is influencing the inter-diffusion phenomena of the materials and consequently the formation of copper compounds. Therefore, the increasing copper phases and diffusion led to a continuous disappearance of the copper concentration after brazing.

However, both joints were free of defects and cracks, showing a homogenised and constant interface simultaneously in tungsten and steel. In addition, the mechanical tests showed that, despite all, the strength of these kind of joints are very high (309 ± 32 MPa without PBHT, and 226 ± 106 MPa with consequent heat treatment [56]) with respect to the others with different filler materials.

According to the promising results, the same authors continued to analyze the W/Cu/steel joint noting that the strength of the joint reduced with the heat treatments applied [57].

The presence of cracks in the W side perpendicular to the interface with the filler material and the presence of some voids, clearly reduced the bond strength.

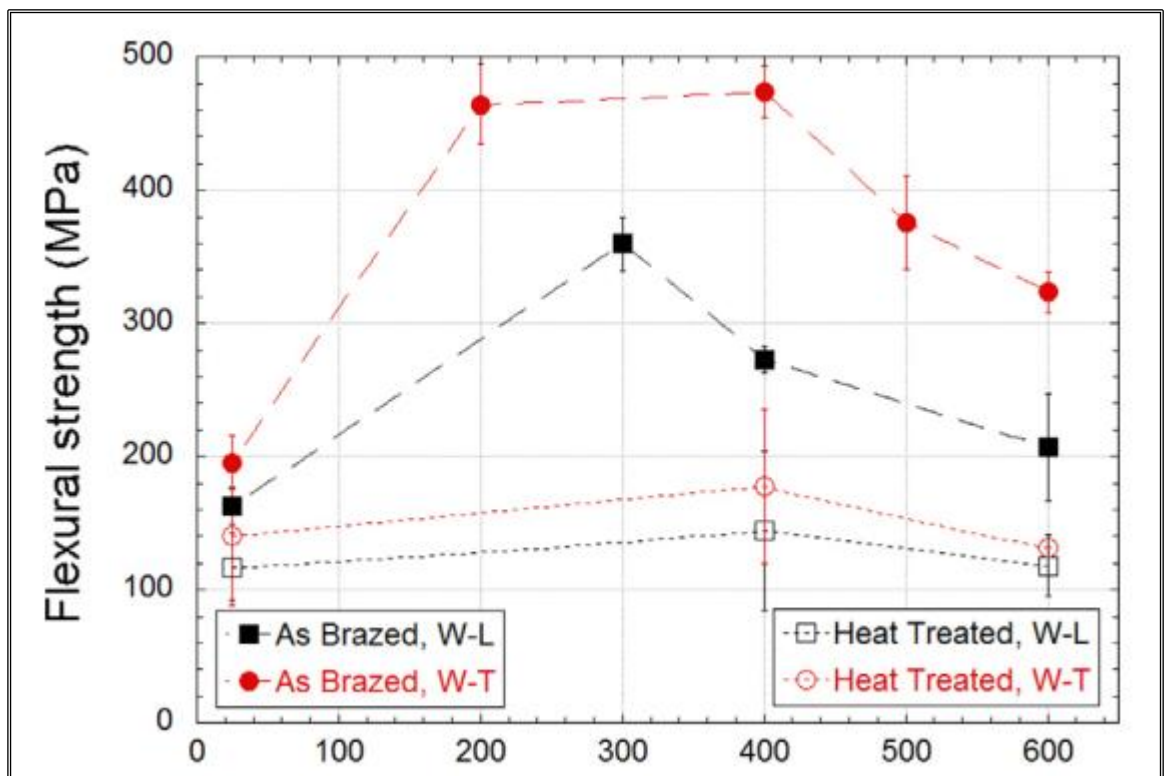


Figure 31: Flexural strength before, and after the heat treatment [57]

As can be seen from the previous figure, after the heat treatment, the Cu was penetrated inside the EUROFER grain boundaries more than the case without PBHT.

Even at low temperatures, the influence of the annealing process decreased significantly the strength of the joint. In particular, the increased penetration achieved the accumulation of voids and the softening at a significant distance of the interface region.

The diffusion of copper inside the steel had as a consequence the formation of a hard layer of 1,5 μm (16 GPa) [57], containing Fe, Cu, and W compounds (Fe_2W , Fe_7W_6), which is considered the weakest part of the joint.

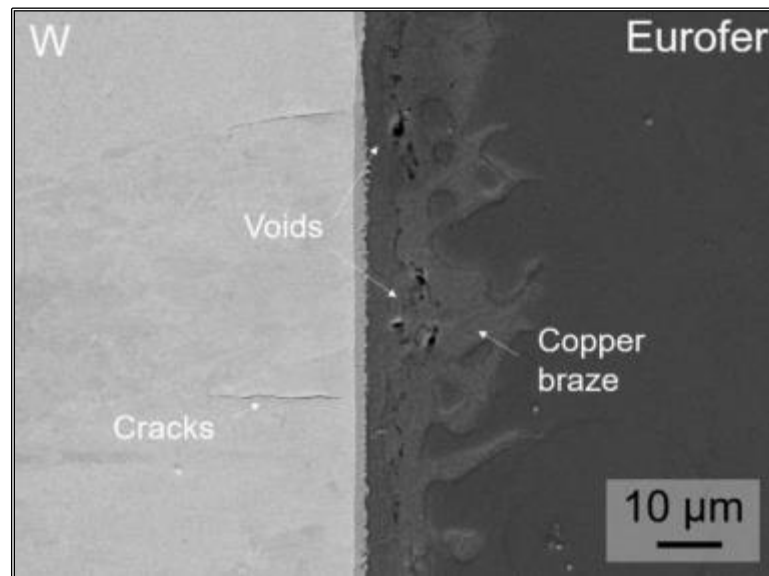


Figure 32: SEM image of the joint after the heat treatment (780°C, 120 min) [57]

From the studies described above, it is noticeable that different materials are being developed in order to achieve a common goal: reliable and strong joints capable to withstand at severe fusion nuclear conditions. The brazing technique represents a well-known joining process, which allows to produce joints with different materials, at low costs. Moreover, the melted filler in the intermediate region ensures a strong and continuous bond. However, it must be said that it is difficult to find a perfect filler material, for example: if Ti is used, during brazing the joints suffer oxidation and production of TiC compounds; if Cu metal filler is used, the diffusion inside the steel grain boundaries causes a softening of the seam region; using Ni as interlayer, the residual stresses can be reduced, but there are some threshold values in relation to its activation with neutrons. Besides, it is also important to highlight the fact that there are not well-established mechanical tests and rules for W/steel joints, so according to the type of material, it is not always easy to compare the different samples. Surely, further investigations are necessary, improving and optimising the parameters of brazing regardless the type of interlayer/filler material chosen and its compatibility with the adjacent substrates.

CHAPTER 3

EXPERIMENTAL STUDY

3.1 Introduction

The development of joining materials plays a key role in the international scenario of fusion energy, because joints represent a fundamental step to complete the components and the assembly of ITER.

As said before, one of the principal problems for W/steel joint is the mismatch between the coefficients of thermal expansion of tungsten and EUROFER or 316L stainless steel, which causes significant residual thermo-mechanical stresses for the bonding.

As reported in literature, it has been noticed that copper shows good mechanical properties, and being a ductile material, it could accommodate the residual stresses caused by the difference in CTEs. Finally, it can be considered a promising solution for W/steel brazed joints. Nevertheless, as J.de Prado et al. [57] noticed, the interdiffusion of copper into the steel grain boundaries during brazing may constitute a problem because it causes the softening of the interface region, and a hard brittle layer decreases the strength of the whole joint. In this regard, this study is focused on W/steel joints using two different joining materials: pure copper and a commercial metal alloy (Gemco®) as filler materials for brazing, with the addition of a magnetron Cr-sputtering layer on the steel surface.

The second objective of this experimental activity is concentrated on modifying the surface of steel samples in order to prepare them for Direct Bonding (DB). The aim is to try a new concept of DB in which, due to the surface modification, it is possible to improve the strength of the joint at the interface region. The modifications were made with a nanosecond laser.

3.2 Materials and methods

The materials used were pure tungsten, 316L stainless steel and EUROFER 97 as base materials for the joints, supplied by *Centro de Investigaciones Energéticas, Medioambientales y Tecnológicas* (CIEMAT, Spain-Madrid). The dimensions of the samples were 1.5 mm x 1.5 mm in the case of EUROFER, and 1.5 mm x 2 mm in the case of steel.

The filler material used was pure copper (>99.95 %) in foils. The thickness of the interlayer ranged from 0.1 mm to 1 mm, in order to test the wettability of the samples with foils of copper of different thickness, and to find the optimum value for brazing.

A second type of filler material was experimented, a commercial Cu-based alloy named Gemco® (87.75 wt% Cu, 12 wt% Ge and 0.25 wt% Ni; Wesgo Metals) [58] in foils of 0.06 mm, to observe the differences in wettability with respect to copper.

For the surface coating of the steel samples, a magnetron sputtering with a Cr target was used, creating three different layer thicknesses (400 nm, 500nm, and 700 nm) to make further investigations and comparisons with reference values found in bibliographic researches [59].

The samples were analysed with optical microscope. The joints were characterised using Field Emission Scanning Electron Microscopy (FESEM- ZEISS Supra 40) with an Energy Dispersive Spectroscopy (EDS- SW9100 EDAX) detector. The steel surfaces for laser texturing were characterised with the same technologies before and after texturing.

In these activities the mechanical tests were not performed. For this reason, the produced joints will be tested with High-Heat Flux tests and will be mechanically characterised at Forschungszentrum Jülich Research Centre (FZJ- Jülich, Germany).

Table 1: Chemical composition (Max. value) of AISI 316L and EUROFER 97 [62][63]

AISI 316L (wt.%)							
C	Mn	Si	Cr	Ni	P	Mo	Other
0.03	2.0	1.0	16.5-18.5	8-13	0.04	2-2.25	N<0.11
EUROFER 97 (wt%)							
C	Mn	V	Cr	Ni	P	Mo	Other
0.120	0.60	0.25	9.50	0.005	0.005	0.005	<0.11

3.3 Brazed joints

3.3.1 Experimental technique

A magnetron sputtering with a pressure of 10^{-4} Pa was utilized to develop three different layers on the steel surface samples. The power employed for the process was of 200 W in DC and the target for coating was of chromium.

More in details, all the parts to be joined were ground down to 2400 grit to prepare and clean the surface of the materials with SiC papers, and polished with an ultra-sonic bath, at 45°C for 10 min, to eliminate all the surface contaminations and prepare the samples for

the brazing treatment.

First, W/Gemco®/steel joints were prepared. The brazing procedure was carried out in a tubular furnace with a continuous Ar flow to avoid the oxidation of the sample. Three foils of metal filler were employed. According to [58], the brazing treatment was carried out at 970°C-980 °C, for 30 minutes, with a heating and cooling rate of 10°C/min. An additional weight of tungsten was put over the sample, in order to maintain the position of the parts involved, during brazing.

Even if the grains of the steel may be coarsened as a consequence of the brazing temperature, no additional post brazing heat treatment was carried out because it goes beyond the aim of this work.



Figure 26: Tubular furnace (Carbolite) of the laboratory at DISAT-Politecnico di Torino

The other type of joining performed was a W/Cu/steel joint. First, 3 foils of copper were chosen to be inserted as filler material. The first thickness of copper was 100 μm but due to the fact that after brazing the resulting sample presented more un-bonded parts, other thicknesses of copper were investigated up to the most suitable for the brazed joint.

It was found that the optimum value for copper was 372 μm , in the form of one interlayer.

In the case of thicker brazing foils, the high spreading capabilities of Cu braze at the brazing temperature gave rise to the exudation of the metallic filler out of the joint

clearance. Sandwich-like joined samples were produced; the tungsten and the steel were both sliced into 1.5 mm x 1.5 mm x 3 mm pieces in the case of joints with EUROFER and 1.5 mm x 2.0 mm x 3.0 mm in the case of joints with steel.

After selecting the optimal thickness, the brazing process was also performed into a tubular furnace under an argon flow, at the following conditions: brazing temperature 1130 °C, for 10 minutes, with a heating and cooling rate of 5°C/min. According to the tubular furnace utilized (Carbolite), to reach a good bonding an additional external pressure on the top of the joint was necessary. In particular, four joints were tested.

Also in case of W/Cu/steel assembly, an external weight of tungsten was used during brazing, with the aim of maintaining in position the base materials and avoiding misalignment of the three materials.

In both cases it was preferable to put the sample of tungsten at the bottom of the joint and the steel on the top for reasons related to the geometry of the tubular furnace. However, several joints were also performed without an additional weight to test and compare the wettability of the two filler materials.

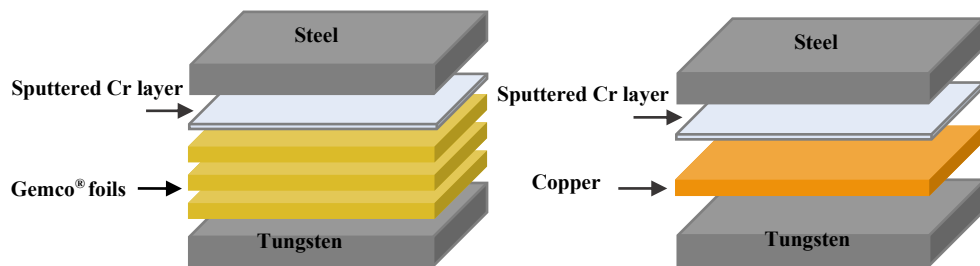


Figure 27: Structures of the performed joints

3.3.2 Results and microstructural analysis

3.3.2.1 W/Gemco®/steel joints

The W/Gemco®/steel joints were successfully produced. According to [57], the weakest part of the W/Cu/steel joint was at the interface region because of the diffusion of copper along the grain boundaries. Being the Gemco® alloy a Cu-based filler material, further investigations were developed in order to reduce the diffusion of copper.

Considering the study of D. Bachurina et al. [53], with the purpose of reducing the content of copper at the seam region, element as Ge and Ti were used because of their low-activation and activities (9.32×10^{-10} and 1.16×10^{-3} Sv/h, respectively) [53].

For this reason, in this work the use of Gemco® alloy as filler material was experimented for both test the wettability of the brazing filler with respect to the base materials, and because the reduced amount of copper together with Ge and Ni, may reduce the diffusion of Cu into the steel.

Moreover, the Gemco® filler alloy presents good thermal conductivity at the interface, fundamental requirement for nuclear fusion joint.

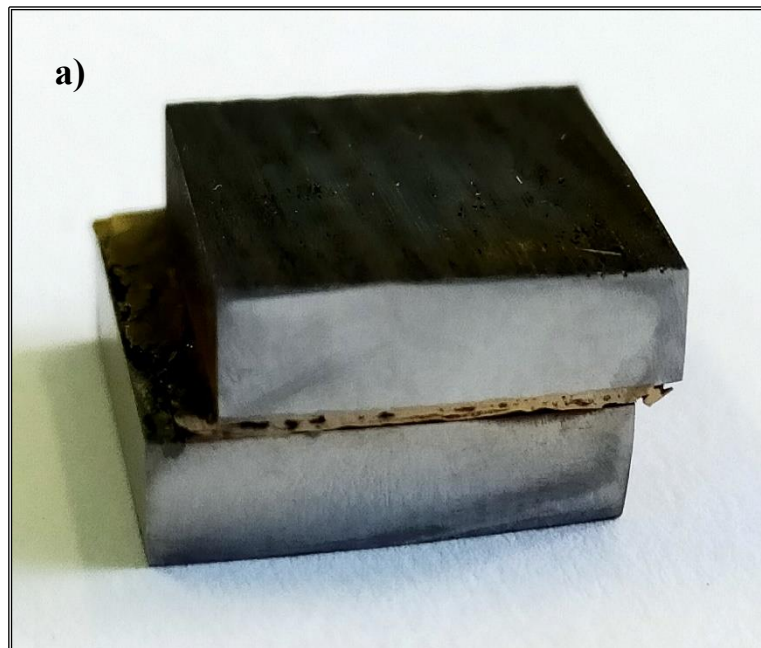


Figure 28: Macrography of sample a of W/Gemco/steel without applying additional pressure during brazing (980 °C) and without coating on steel surface

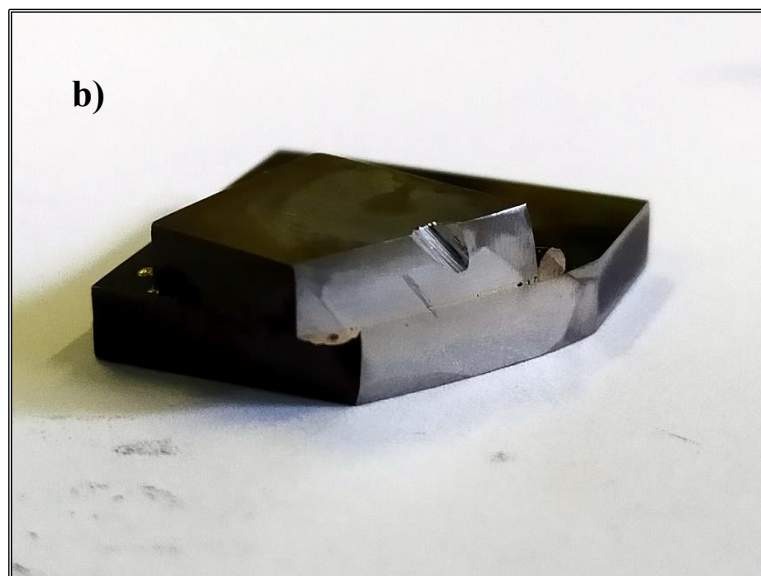


Figure 29: Image of sample b of W/Gemco®/steel joint with additional pressure (weight of W) during brazing (980°C) and sputtering of 400 nm.

In the first experimental activity two samples were produced: **sample a**, free of a Cr coating on steel surface, and **sample b** provided of a sputtered Cr layer (see fig 36). From the previous figures it is possible to observe the differences at the interface of the joints.

The wettability of the brazing filler alloy with respect the base materials changed according to the pressure; the first sample (without sputtering) is showed in fig. 34 and presents un-bounded regions, pores, and voids (in particular at the W side) that can be observed by the naked eye. This can be attributed to the lack of an additional external pressure during brazing (see fig.37). This explanation was confirmed by the second sample (with a Cr magnetron sputtering on steel of 400 nm) represented in figures 35 and 38, in which it is possible to notice a section of the joint in which the interface is clearly more homogeneous and free of voids.

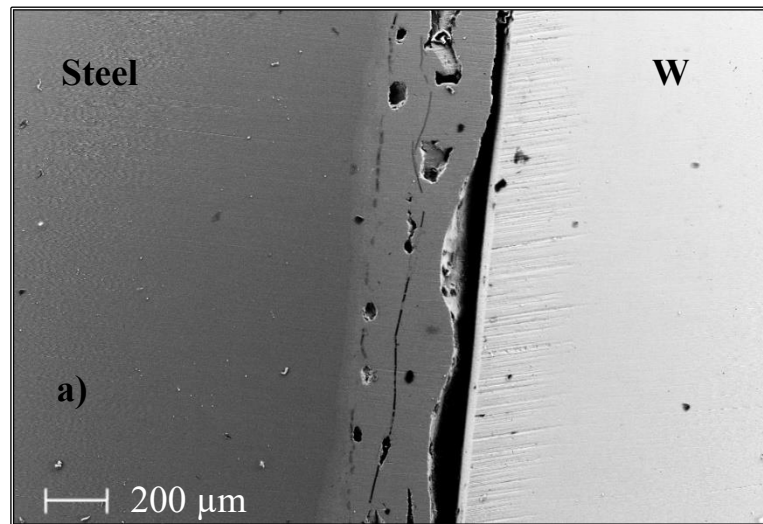


Figure 30: FESEM image of the sample a at high magnification

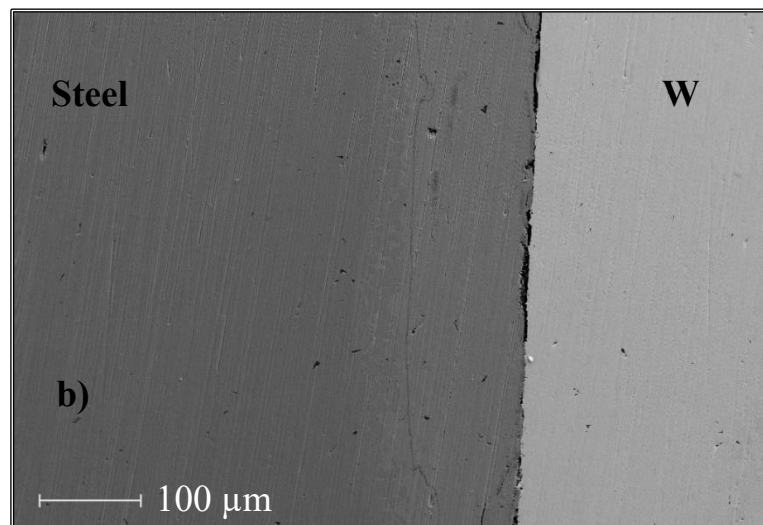


Figure 31: FESEM image of the sample b at high magnification

These samples were compared in order to understand if the presence of chromium on the steel surface substrate was influencing the diffusion of the Cu-based alloy into the grain boundaries.

From the early analyses of Energy Dispersive Spectrometry (EDS) the microstructures of the steel surfaces were analyzed, to confirm the presence of chromium in layer on the substrates.

The first sample, sputtered with a Cr layer of 400 nm, presented the typical cauliflower structure of a surface coating by magnetron sputtering. The second one (sputtering of 500 nm) and the third (sputtering of 700 nm) instead, exhibited very particular configurations, as fig. 32 shows. Images reported in figure 32 refer to top view of coated samples.

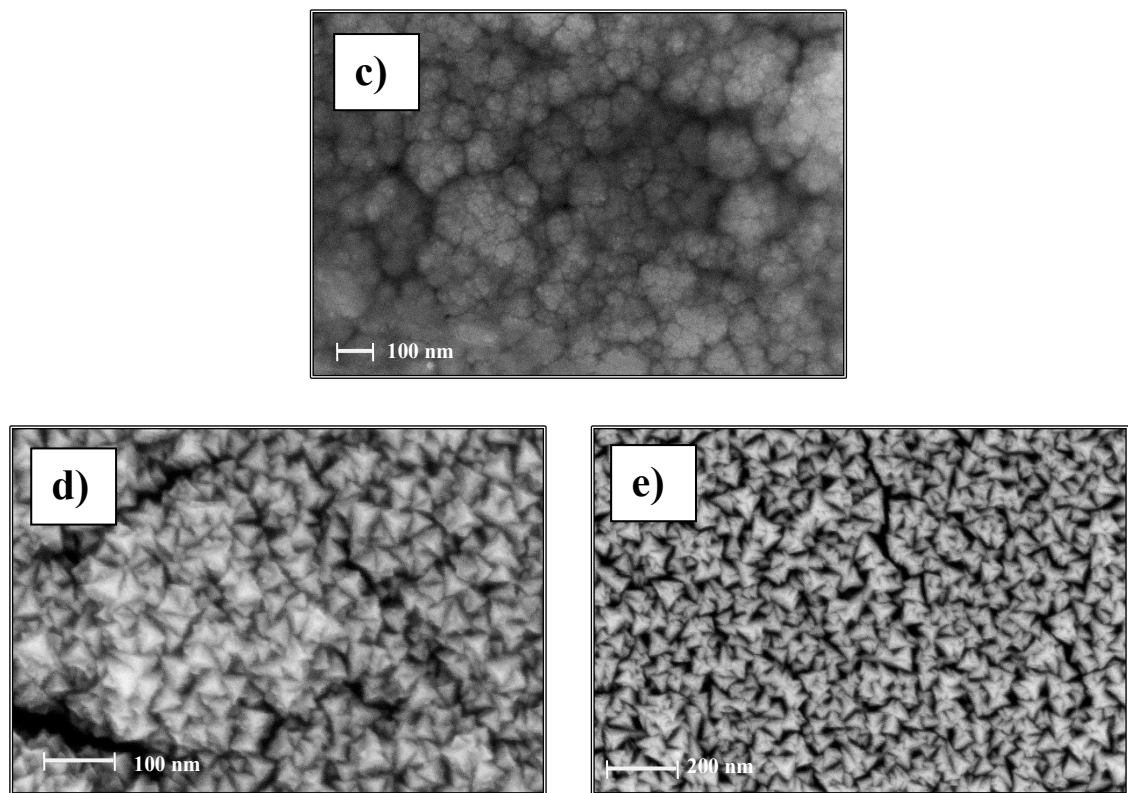


Figure 32: FESEM images of c) steel surface with 400 nm of Cr sputtered, d) steel surface with 500 nm of Cr sputtered, e) steel surface with 700 nm of Cr sputtered

From compositional analysis by EDX, a significant amount of oxygen was detected in the coating. It is probably due to a vacuum loss in the sputtering apparatus. However, the coating resulted in a homogeneous layer, not fully dense but with a well-defined microstructure. This is important because the presence of a homogeneous Cr coating on the steel surface could reduce the diffusion of Cu inside the steel grain boundaries.

It represents a physical barrier for Cu. Moreover, it can be interesting to make further investigations in order to better understand how the atoms combined and formed these microstructures.

Returning on the W/Gemco®/steel joints, FESEM and EDS investigations were carried out. Also here, a comparison between the samples with and without sputtering was performed to understand if the presence of Cr influenced the metal filler alloy diffusion.

In both samples a good diffusion of the Gemco® in the seam zone was detected, indicating a good metallic melting of the brazing filler. A positive metallurgical bond was achieved at the steel/Gemco® interface in both cases, despite the voids and pores. However, the images revealed less contact between the tungsten and the intermediate Gemco® alloy; this critical aspect can be explained by the higher difference in CTE between the brazing alloy and the W plate if compared to the CTE difference between the braze and the steel plate.

As said before, surely the presence of a tungsten weight influenced the bonding of the joint, but it is important to say that additional investigations are necessary, in order to better understand if the chosen Cu-based alloy could represent a good candidate for high-temperature joints in nuclear applications.

The EDS analysis showed that germanium was present at the seam region, specifically at the steel/Gemco® interface. More in details, comparing the two W/Gemco®/steel joints produced, in **sample a**, a higher amount of Ge was found far from the interface, with respect to **sample b**, which was equipped with a Cr coating. This demonstrated the utility of the metallic layer.

In both joints a certain amount of copper was found far from the interface, but EDS analyses confirmed that the concentration of Cu was higher in the first joint. A deeper characterization at the tungsten side is necessary because, due to the low content of metallic particles, the EDS analysis did not provide significant results.

The morphological characterisation of the joints indicated a better bonding at the W/Gemco® interface in sample b. This because of an additional weight of tungsten during brazing. Moreover, as said before, a section of sample b was analysed considering the internal portion of the joint that, in general, presents a more uniform interface.

Sample a, instead, was produced without an additional weight of tungsten (during brazing) and its morphology was characterised starting from the boundaries of the specimen, in which the probability to find defects is higher than the internal part.

More in details, both W/Gemco®/steel joints were compared from the point of view of diffusion elements.

Sample a, without sputtering, exhibited a diffusion of the brazing filler up to $\sim 30 \mu\text{m}$ at the steel/Gemco[®] bonding side; **sample b** showed an infiltration of the Gemco[®] alloy at the same interface up to about $22 \mu\text{m}$.

These results confirmed the fact that the presence of the sputtered Cr layer on the steel surface substrate is influencing the diffusion of the filler material, reducing the infiltration in the steel grain boundaries; tailoring the thickness of the sputtered Cr layer, the diffusion of copper can be controlled. The Cu diffusion, in fact, has detrimental effects on the mechanical properties of the joint (because of the softening at the interface region) and may cause problems during the reactor operation conditions (due to the difference in melting temperature).

Moreover, from the FESEM images it is also possible to observe a good diffusion of the filler material at the steel/Gemco[®] interface, indicating a well-bonded joint. It is possible that at the seam region a reaction layer comprising brittle intermetallic compounds and phases is formed; a Micro X-Ray diffraction analysis is recommended to better understand the formation of this reaction layer. Nevertheless, the presence of reaction layers leads to an increasing hardness of the joint and to a consequent decrease in strength. At the moment, this layer cannot be detected (in contrast with what observed in [40] and [56]) or it can be supposed that it is very thin.

From the maps below it is possible to observe the diffusion of the relevant elements into the base materials of sample b.

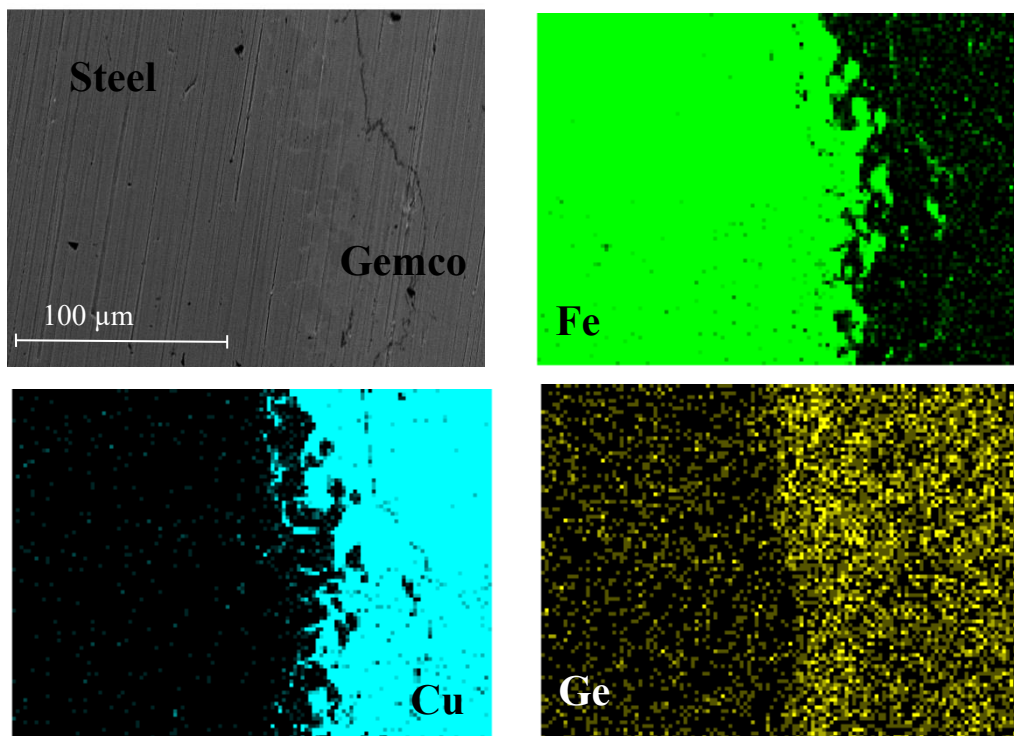


Figure 33: Elemental maps at the steel/Gemco[®] interface (sample b)

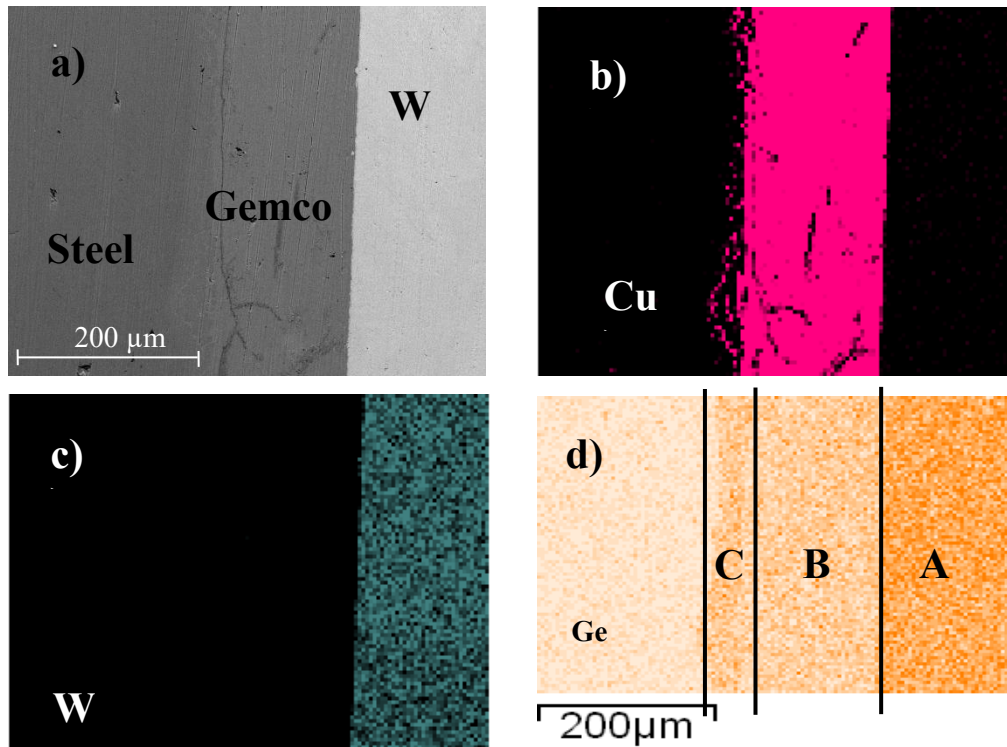


Figure 34: Elemental maps of the W/Gemco®/steel interface (sample b)

From fig.33 the diffusion of Cu and Ge inside sample b is visible. Most of germanium was found at the steel/Gemco® interface as expected; the copper, instead, diffused through the steel grains, and not inside the tungsten.

Moreover, fig.34 shows that no Cu was detected at the W side of the joint. In addition, it must be highlighted that, in fig. 34 (d) Ge presented different solubility in the joint and three different areas were considered: **A** indicating the tungsten zone, **B** indicating the interface (filler) zone, and **C** which is a small area in proximity of the steel/Gemco® interface.

The A zone presented the higher amount of Ge particles, indicating a high solubility of the latter inside the tungsten; the second zone (B) was characterised by the lower amount of Ge in the interface zone, and the C zone represented a small area full of Ge particles, in proximity of the steel/Gemco® interface. It could be interesting to explore how germanium interacts with the base materials, because the results indicate that Ge may be stopped at steel/Gemco® interface by the Cr layer. This could also demonstrate the effect of the sputtered Cr layer. Moreover, additional studies are necessary to understand the relation between Ge and W, as regards their solubility; bibliographic research has been carried out on this topic, but, to the best of author's knowledge, no data are supplied in literature.

In any case, from micrograph observation coupled to EDS analysis, it can be supposed that the solubility of Ge in W is high, thus leading to a depletion of this element from the brazed area. However, further investigations are needed, especially from a thermo-

mechanical point of view. It will be necessary to prove the feasibility of W/Gemco/®steel, but is reasonable to say that the Gemco® alloy, presenting a lower amount of copper and consequently reduced diffusion of copper into the facing substrate, could represent a promising solution for nuclear fusion joints.

3.3.2.2 W/Cu/steel joints

High-temperature joints with Cu as interlayer have been studied for a long time, due to the high ductility of copper that can accommodate the residual stresses at the interface, caused by the CTEs mismatch between tungsten and steel (or EUROFER).

For this reason, in this work a W/Cu/steel joint is investigated with the addition of a layer of Cr on the surface steel to be joined, deposited by magnetron sputtering, as barrier.

The aim of the joining is to understand if the presence of chromium influences the diffusion of copper inside the steel grains, in order to avoid a softening area that reduces the general strength of the joint, and constitutes a detrimental factor for the joint mechanical properties.

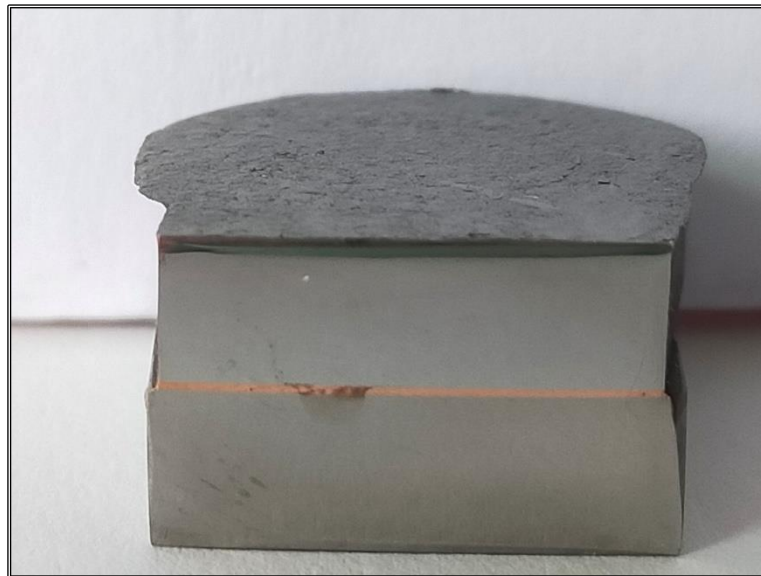


Figure 35: Image of the W/Cu/steel joint (1130°C) with 700 nm sputtering

From fig.35, it is possible to observe the W/Cu/steel joint (1130°C) with a sputtered Cr coating of 700 nm, in which the interface is free of defects or voids; this indicates that the copper used as interlayer in form of 1 foil (372 μm) presented a good wettability with both the base materials. In particular, no un-bonded regions were detected, even at the tungsten interface.

The joint was performed successfully, reaching a good metallurgical bonding according to previous works in which W/Cu/steel joints were investigated [56 - 59].

All the cross-sections of the joined samples showed high continuity along both interfaces, which indicated that the braze has correctly melted at the brazing temperature, spreading and filling all the surface roughness and the joint clearance.

A deeper analysis was experimented in order to observe the changes in microstructure and composition, with the addition of a 700 nm layer of Cr. The thickness of 700 nm was chosen because the sputtered Cr layer seemed to be more homogeneous.

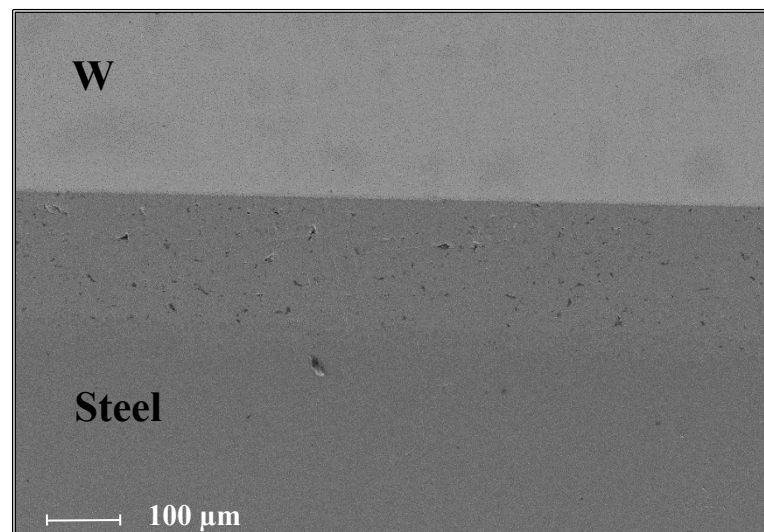


Figure 36: FESEM image of the whole W/Cu/steel joint (sputtered 700 nm)

Fig. 36 shows the interface region of the joint at FESEM low magnification, confirming the previous statements.

The joint is well-bonded and the seam both at steel and W interface is defect-free. Besides, the diffusion of Cu is well recognisable (see fig. 37) in the intermediate region of the joint, indicating that copper reacted well with the base materials and it presents high wettability.

Fig. 37 shows a higher magnification of the steel/copper interface where it is possible to observe the diffusion of copper inside the grain boundaries of the steel.

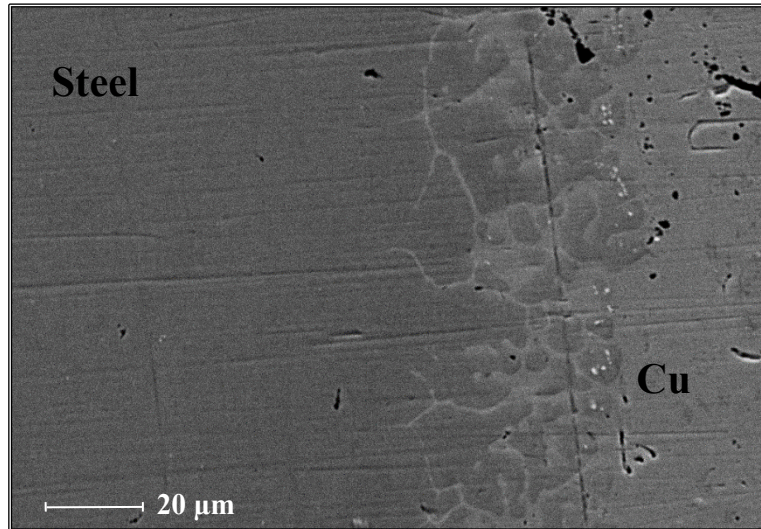


Figure 37: Steel/Cu interface of the W/Cu/steel joint (sputtered 700 nm)

Using the EDS technology, the chemical composition of the interface was carried out. More in details, this study is focused on the diffusion of copper through the steel, so mainly the steel/copper interface was investigated.

The diffusion path of the copper inside the steel grains was about 40 μm . In order to compare this result with the case in which a W/Cu/steel joint was not provided of a Cr sputtered layer, the study of J. de Prado et al. [57] was taken into account, considering their data as reference values. The authors performed a W/Cu/steel joint without Cr layer.

They reported a diffusion of the copper at the steel/Cu interface of 20 μm , using a thickness for the Cu metal filler material of 50 μm . Besides, the tungsten substrate was not influenced by diffusion phenomena of copper.

In this experimental activity, a foil of 372 μm of Cu was used for brazing. EDS analysis confirmed the fact that at the W/Cu interface region no copper diffusion phenomena were present. Instead, at the Cu/steel interface, it is possible to say that the presence of chromium on the surface of the steel substrate seemed to effectively work, because in terms of proportions (comparing the metal filler thickness and Cu diffusion) the copper diffusion in our experimental activity was less than the reference values.

Nevertheless, it must be emphasized that to compare the results of this work it is necessary to experiment the brazed joints with the same thickness of Cu interlayer, so it has to be verified.

Considering the Cu/steel interface, bibliographic research [57] demonstrated that in this region an inter-diffusion layer was formed, leading to a softening of the seam area.

Besides, the layer was brittle (high content of Cr, Fe, and W) and consequently presented the higher hardness of the whole joint.

The following table highlights the chemical content of Cr, Fe, and Cu, at the steel/Cu interface region, and the subsequent figure shows the relative EDS analysis.

Table 2: Chemical composition at Cu/steel interface

Element	Weight%	Atomic%
Cr	5.96	6.59
Fe	66.39	68.38
Cu	27.65	25.03

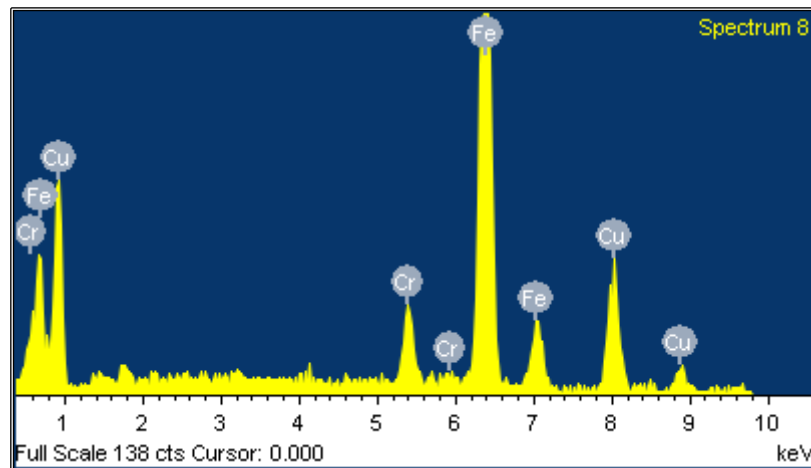


Figure 38: EDS spectrum at Cu/steel interface

It is evident that copper was still present and diffused at the grain boundaries of the steel grains even with the presence of chromium. However, as said before, the diffusion seemed to be reduced.

In fact, from the maps below it is noticeable that the copper diffused well along the steel grain boundaries, and no copper particles were detected far from the interface. Besides, iron did not diffuse towards the filler material, the low amount of Fe detected at the interface is too low to be considered significant for the analysis.

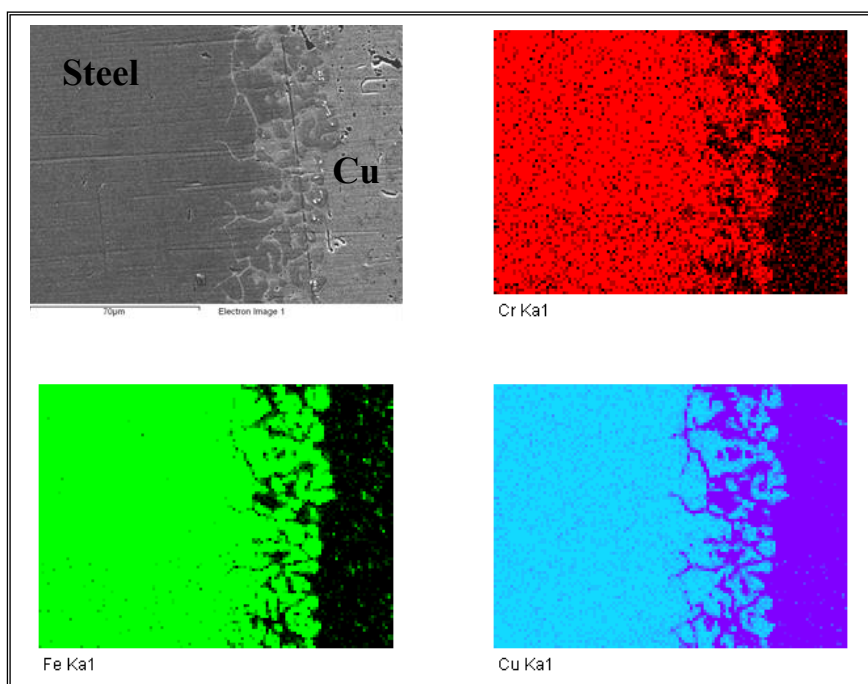


Figure 39: elemental maps of the steel/Cu interface

Moreover, the chromium detected with EDS analysis seemed to be distributed in steel region, as expected. In the filler region, a certain amount of Cr was detected, probably due to the fact that at the steel/Cu interface a coating of Cr was deposited. However, the amount is too low to be considered relevant in terms of microstructure.

In general, the presence of the Cr coating did not influence the metallurgical bonding of the whole joint, fundamental requirement for the heat transfer in operation conditions of fusion nuclear reactors.

W/Cu/steel joints, so as W/Gemco®/steel joints, after the microstructural characterisation were prepared to be sent at Forschungszentrum Jülich Research Centre (FZJ- Jülich, Germany), and to be subjected to further investigations from a thermo-mechanical point of view.

Finally, High-Heat flux tests will be carried out to experiment their resistance under fusion nuclear environment.

3.4 Surface modification of steel

The use of laser as engineering solution for the modification of the surfaces of metals is becoming one of the most promising technique for fabrication of components, both for joining and for repairing activities. The variation in surface morphology of materials leads to improvements from different points of view.

With laser it is possible to act on various geometries, from the simplest one to the most complex shape. For this reason, laser texturing represents an important tool in case of maintenance scenarios [60].

Moreover, it must be emphasized that the effects of surface modification on metals are significant for the performances of the component that they will constitute. In general, one of the most important improvement is related to the enhancement of tribological and friction properties.

The formation of micro-dimples on the steel surface affects the roughness of the substrate and consequently also affects the adhesion properties. In the case of joining technologies these developments are fundamental, in particular for direct bonding.

Furthermore, laser texturing is widely used in industries also to enhance the wear resistance and the load capacity [61] of components.

During the last years different laser technologies have been developed, which are focused on the surface manufacturing of metals with pulsed lasers. Specifically, nanosecond, picosecond and femtosecond pulsed lasers are widely employed.

In this direction, Peter Šugár et al. [61] noticed a significant influence of the laser beam pulses on the superficial mechanical properties of the material, on the shape, and on the dimensional accuracy of the component to be produced.

As said before, the direct bonding joining does not constitute a promising technology for high-temperature fusion joints because of the low strength and resistance of the resulting joints.

The present activity is centered on the modification of stainless-steel samples, in order to improve the friction conditions, to increase the bonding surface, to enhance the interlocking at the interface and consequently the mechanical properties of tungsten-to-steel direct joint.

3.4.1 Experimental activity

Three sample of stainless steel were considered, in order to obtain three different superficial textures respectively. The specimens had dimensions of 1.5 cm X 1.5 cm. Before of the texturing they were ground down to 4000 grit (gradually) with SiC papers, and finally polished with an ultra-sonic bath for 10 minutes at 45°C, to eliminate any type of external contamination.

After that, the samples have been assigned to LINKS FOUNDATION laboratory, in collaboration with the Politecnico di Torino, in order to perform the laser texturing of these samples.

A nanosecond pulsed laser (10^{-9} s) was used to fabricate the textures on the steel surfaces.

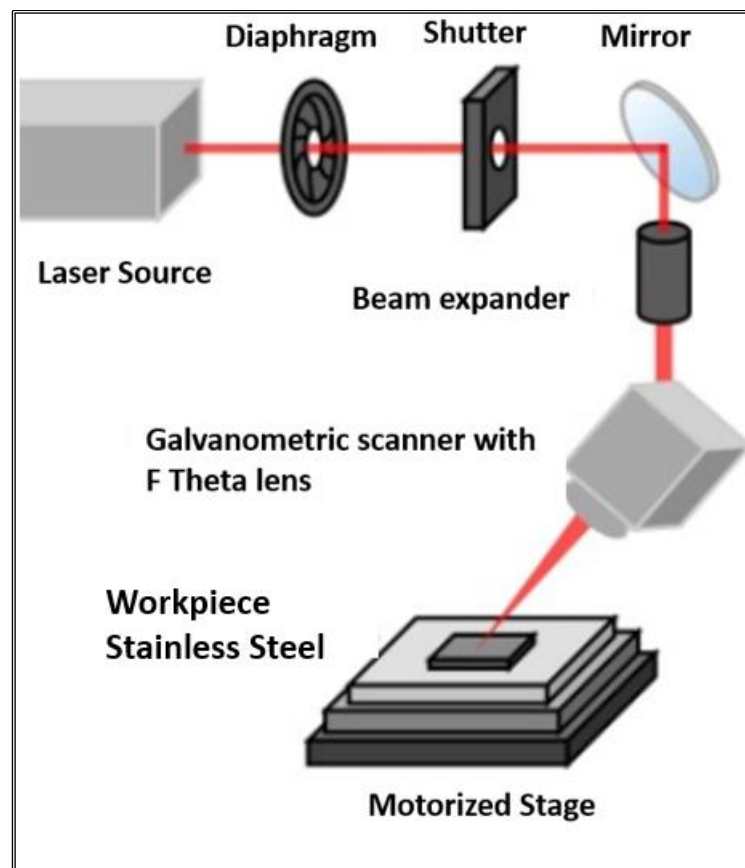


Figure 40: Scheme of the laser texture procedure

To differentiate the patterns of the texture, different power ranges were chosen.

The laser frequency was of 20 kHz, with a scan speed of 3 mm sec^{-1} . The micro-dimples produced on the surface of stainless steel have been set in the form of cross lines, with one repetition.

The textures were fabricated with cross lined patterns spaced at 40 μm .

The three stainless steel samples were experimented, so as to create dissimilar texture for each sample.

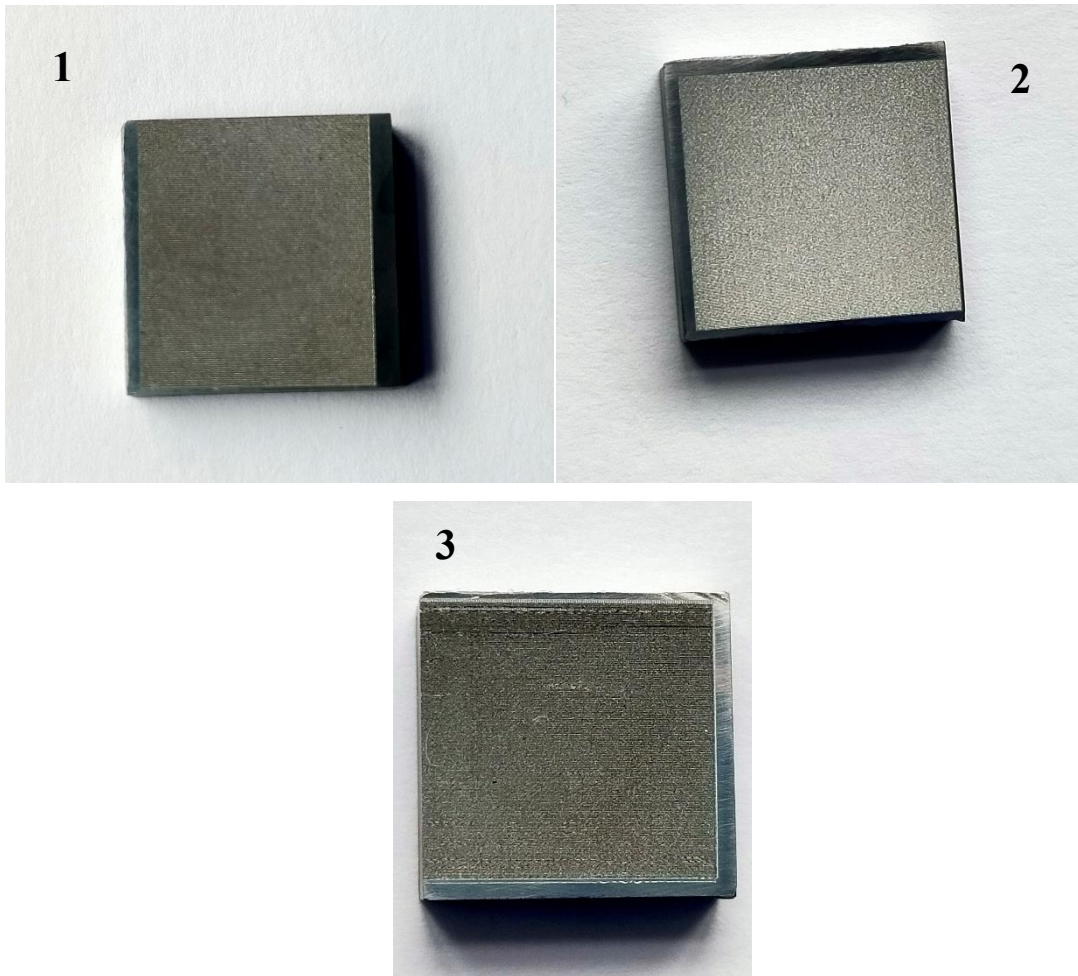


Figure 41: Images of laser textured steel samples (1.5 x 1.5 x 2 mm)

The samples were textured with varying power, in particular sample 1 with 85% of the total power (20 W average), sample 2 with 65%, and sample three with 100%.

According to the power data, three different values of fluence were utilised: 30 J/cm^2 for the first sample, 23 J/cm^2 for the second, and 35.3 J/cm^2 for the last one.

Due to the fact that the texturization process was carried out without protective atmosphere, sample 1 was subjected to a post texture treatment, in order to eliminate the superficial oxide layer.

For the removal of the oxide layer, a bath of acid acetic was chosen because it presented characteristics that were less aggressive for metals.

During the acid bath, the sample was heated by a heating plate for 30 minutes at a temperature of 80°C, to accelerate the removal chemical reaction.

Once clean from oxide, sample 1 and the other samples (no post texture treatments) were characterised by FESEM analysis and their superficial composition was investigated by EDS technology.

FESEM analysis showed well-textured steel samples, as fig. 42 shows.

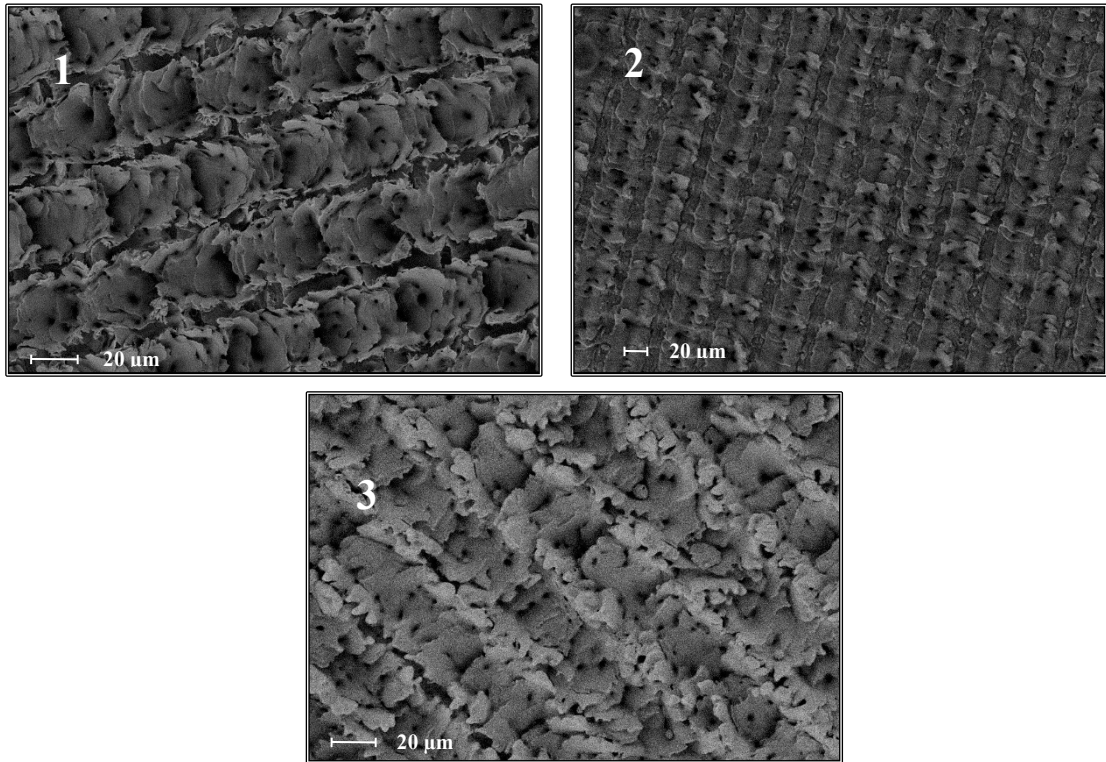


Figure 42: Top view FESEM images of the surface treated steel samples

The FESEM analysis gave a first confirm for the removal of the oxide layer from the surface of sample 1, but further investigations with EDS technology were carried out.

In fact, from the following tables it is possible to notice that the EDS spectrum detected the presence of superficial oxygen in sample 2 and 3, and the first sample, which was subjected to post acid treatment, was free of oxygen.

After these confirmations, the rest of the samples were treated as the first with acid treatment to eliminate the oxide, and to be prepared for a future direct bonding with tungsten.

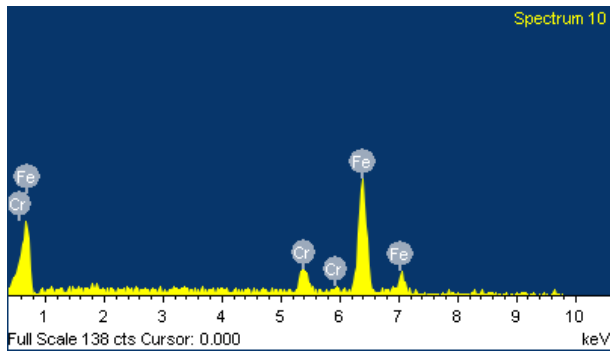


Figure 43: EDS spectrum of sample 1

Element	Weight%	Atomic%
Cr	10.22	10.90
Fe	89.78	89.10

Table 3: Weight and atomic concentrations of sample 1 (EDS)

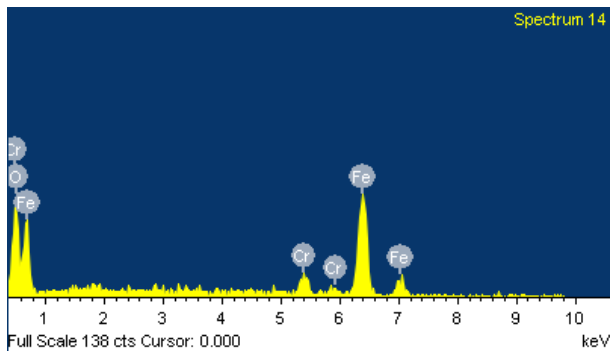


Figure 44: EDS spectrum of sample 2

Element	Weight%	Atomic%
O	17.08	41.68
Cr	7.17	5.38
Fe	75.75	52.94

Table 4: Weight and atomic composition of sample 2 (EDS)

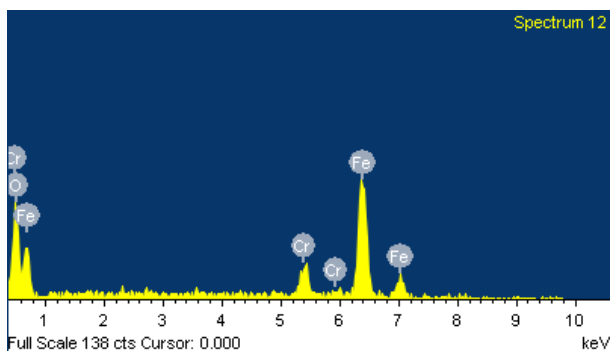


Figure 45: EDS spectrum of sample 3

Element	Weight%	Atomic%
O	14.50	36.99
Cr	9.51	7.47
Fe	75.99	55.54

Table 5: Weight and atomic composition of sample 3 (EDS)

In general, the resulting textures presented homogeneity and repetitiveness; the texturization leads to an increasing surface exposed to the joint which may enhance the contact area for direct bonding. Increasing the contact area, the direct bonding of tungsten and steel should improve.

Finally, the treated steel specimens were prepared to be bonded with tungsten.

Further investigations are needed in this direction, because to understand and prove the joining improvement for W/steel direct bonding, it is necessary to submit them to mechanical tests. In the present thesis mechanical tests on direct joints were not carried out because of the difficult availability of tungsten samples.

However, it is important to say that these joints may constitute a real base for future investigations and developments on direct bonding for nuclear fusion applications.

CONCLUSIONS

This thesis is divided into two fundamental parts: one regarding bibliographic research on nuclear fusion joining, and the second one which is experimental and was carried out within the Galance (Glasses Ceramics and Composites) Group at Politecnico di Torino. The aim of the experimental part was to produce tungsten-to-steel brazed joints with the use of Cu or commercial Cu-based alloy (Gemco®) as filler materials, and to modify the surfaces of steel samples in order to improve the W/steel joints performances (in case of direct bonding). More in details, for samples used in brazing joining process, the surfaces of the steel substrates were coated with a Cr layer by a magnetron sputtering, to create a barrier for the copper diffusion through the steel grain boundaries.

The manufactured brazed joints were W/Cu/steel and W/Gemco®/steel, and they were characterised from a microstructural point of view by SEM and EDX analysis. Mechanical tests were beyond the purpose of the present work.

W/Gemco®/steel joints were performed successfully. A diffusion layer formed at the steel/Gemco® interface region, indicating a good bonding between the filler material and the steel. At the W/Gemco® interface, instead, the brazing filler seemed to have lower adhesion with tungsten, in both the joints produced (one coated with a sputtered Cr layer and the second without coating). Moreover, the compositional maps revealed that, in the case of the W/Gemco®/steel joint where the steel part was coated by sputtered Cr, the diffusion of Cu and Ge was reduced, indicating that the Cr coating is effective in hinder Cr diffusion path. However, the two samples analysed were produced with an important difference: the presence of a tungsten weight during brazing which influenced the wettability of the filler with the adjacent base materials. As a consequence, it is reasonable to say that additional investigations are needed in order to understand if the Gemco® alloy can effectively constitute a promising brazing filler metal. Another important consideration is related to the solubility of Ge. It was noted that Germanium presents a high solubility with tungsten and steel, and as consequence significant amount of Ge was detected in the W side and at the steel/Gemco® interface.

W/Cu/steel joints were fabricated and analysed as well. From a complete bibliographic research, brazing parameters have emerged and were considered as reference values to compare them with the experimental data carried out in laboratory. The presence of a Cr coating on the steel surface influenced the diffusion of the copper along the steel grain boundaries. More in details, from the FESEM analysis and from the maps, it is possible to observe that the Cu diffusion path was about 40 µm into the steel plate of the joint.

According to the reference values in literature, in which a Cu interlayer was used to perform W/Cu/steel joints without a sputtered Cr layer, the present results seem to be promising. In fact, the reference value for the thickness of the Cu interlayer was about 50 μm and in this experimental activity the optimal filler thickness found was 372 μm . The diffusion after brazing, at the same conditions, was 20 μm and 40 μm respectively. This result could be considered as positive, because in terms of proportion, the amount of copper diffused along the steel grain boundaries is reduced and the effect of the sputtered Cr coating can be considered effective.

In general, additional samples are necessary in order to produce and better understand the behavior of the Gemco® filler alloy, and if the presence of Cr on the steel surface is effectively working. Due to the difficult availability of tungsten base material, few joined samples were produced.

A second experimental activity consisted in the superficial modification of the steel by a nanosecond laser. During the texture, due to the fact that the texturization was carried out without protective atmosphere, an oxide layer formed; for this reason, the samples were subjected to an acid-based post texture treatment. At the end, the samples were characterised before and after the texture with FESEM analysis and their superficial composition was investigated by EDS technology.

The aim was to prepare the steel base material for a future direct bonding with tungsten, in order to mechanically test the joints and verify if their performances improved. Texturing may enhance the contact area between the base materials, leading to an improvement of the direct bonding.

Finally, the brazed joints will be sent at Forschungszentrum Jülich Research Centre (FZJ- Jülich, Germany), to be subjected at High-Heat flux and mechanical tests.

BIBLIOGRAPHY

- [1] Jeffrey P. F., *Plasma Physics and Fusion Energy*, Massachusetts Institute of Technology.
- [2] K. Linga Murty and Indrajit Charit, *An Introduction to Nuclear Materials, Fundamentals and Applications*.
- [3] M. Zakaria et al., *Innovative Technology and Instrument to Explore the Risk of Applying High Gamma Radiation Doses on the Nanostructure Surface of the Bones*, *Proceedings of the NSFS XV conference in Ålesund Norway (2008)*, 264.
- [4] <https://www.iter.org/mach/tokamak>
- [5] <https://www.iter.org/mach/magnets>
- [6] <https://www.iter.org/mach/vacuumvessel>
- [7] B. Doshi et al., *ITER Cryostat team, ITER Cryostat—An overview and design progress*, *Fusion Engineering and Design* 86 (2011), Vol. 86,1924–1927.
- [8] <https://www.iter.org/mach/cryostat>
- [9] <https://www.iter.org/mach/blanket>
- [10] https://www.ingegneriadellenergia.net/tematiche/energia_1/
- [11] M. Merola, *The ITER Project and its Plasma-Facing Materials*, Politecnico di Torino, 16 nov. 2020.
- [12] V. Casalegno et al., *co-sputtered w/fe interlayers for joining tungsten to steel*, Politecnico di Torino, XXIV AIV Conference 2019.
- [13] M.Merola, et al., *Overview and status of ITER internal components*, *Fusion Engineering Design* (2014), Vol.89, 890-895.
- [14] W. W Basuki et al., *Investigation of tungsten/EUROFER97 diffusion bonding using NB interlayer*, *Fusion Engineering and Design* (2011), Vol.86(9), 2585-2588.
- [15] https://www.visotticacomotec.com/wp-content/uploads/2019/02/Visottica-Materials-Datasheet_AISI316LS-AISI316L.pdf
- [16] D. Bachurina et al., *Overview of the mechanical properties of W/steel brazed joints for the DEMO Fusion Reactor*, *Metallurgy Journal* 11(209).
- [17] <https://www.tav-vacuumfurnaces.com/blog/22/en/vacuum-brazing> .

- [18] Pergamon Materials Series, Vol. 12, 2007, Chapter 7-Diffusional Transformation, pages 584-587. <https://www.sciencedirect.com/science/article/pii/S1470180407800605> .
- [19] B.Bernal, M. H. Hot Isostatic Pressing (HIP) technology and its applications to metals and ceramics. *Journal of Materials Science* (2004), 39(21), 6399–6420.
- [20] Y. F. Yang et al., Spark plasma sintering and hot pressing of titanium and titanium alloys. *Titanium Powder Metallurgy* (2015), 219–235.
- [21] A.H. Taheri et al., Thermo-elastic characterization of material distribution of functionally graded structures by an isogeometrical approach, *International Journal of Solids and Structures* (2013), Vol.51, 416-429.
- [22] S. Heuer et al., Microstructural and micromechanical assessment of aged ultra-fast sintered functionally graded iron/tungsten composites (2020), *Materials & Design*, Vol.191, 108652.
- [23] W. W. Basuki et al., Investigation on the diffusion bonding of tungsten and EUROFER97. *Journal of nuclear materials* (2011), 417(1-3), 524-527.
- [24] A. von der Weth, et al., Optimization of the EUROFER uniaxial diffusion weld. *Journal of Nuclear Materials* (2007), 367–370 1203–1207.
- [25] T.Hirose et al., Joining technologies of reduced activation ferritic/martensitic steel for blanket fabrication. *Fusion Engineering and Design* (2006), Vol.81, 645-651.
- [26] Y. Junget al., Interfacial microstructures of HIP joined W and ferritic–martensitic steel with Ti interlayers, *Fusion Engineering and Design* 88 (2013) 2457–2460.
- [27] J. Wang et al., Effect of Ti interlayer on the bonding quality of W and steel HIP joint, *Journal of Nuclear Materials* (2017), Vol. 485, 8-14.
- [28] J. Park et al., Joining of tungsten to ferritic/martensitic steels by hot isostatic pressing, *Journal of Nuclear Materials* (2013), Vol. 442, S541-S545.
- [29] W.Liu et al., Fabrication of W/steel joint using hot isostatic pressing with Ti/Cu/Ti liquid forming interlayer, *Fusion Engineering and Design* (2018), Vol. 135, 59–64.
- [30] J. Wang et al., Effect of deuterium on bonding quality of W/Ti/Steel HIP joints in first wall application, *Fusion Engineering and Design* (2019), Vol. 138, 313–320.
- [31] Y. Jung et al., HIP Joining of Tungsten Armor to Ferritic-Martensitic Steel with a Zirconium Interlayer, *Fusion Science and Technology* (2017), 523-529.
- [32] J. Zhang et al., Effect of holding time on the microstructure and strength of tungsten/steel joints by HIP diffusion bonded using a Cu interlayer, *Materials Letters* (2019), Vol.261,126875.

- [33] Y. Wang et al., *Interfacial structure and formation mechanism of tungsten/steel HIP diffusion bonding joints using Ni interlayer*, *Journal of Manufacturing Processes* (2020), Vol. 52, 235–246.
- [34] E. Sal et al., *Joining of self-passivating W-Cr-Y alloy to ferritic-martensitic steel by hot isostatic pressing*, *Fusion Engineering and Design* (2021), Vol. 170, 112499.
- [35] J. Matějíček et al., *Overview of processing technologies for tungsten-steel composites and FGMs for fusion applications* (2015), *NUCKLEONIKA* 60, 267-273.
- [36] S.Heuer et al., *Atmospheric plasma spraying of functionally graded steel/tungsten layers for the first wall of future fusion reactors*, *Surface and Coatings Technology* (2019), Vol. 366, 170-178.
- [37] S. Heuer et al., *Microstructural and micromechanical assessment of aged ultra-fast sintered functionally graded iron/tungsten composites*. *Materials and Design* (2020), Vol. 191, 108652.
- [38] S. Heuer et al., *Aiming at understanding thermo-mechanical loads in the first wall of DEMO: Stress–strain evolution in a EUROFER-tungsten test component featuring a functionally graded interlayer*, *Fusion Engineering and Design* (2018), Vol. 135, 141–153.
- [39] J. de Prado et al., *Study of the Fe-Ti/W system for joining applications in high-temperature fusion reactor components*, *Fusion Engineering and Design*. (2016), Vol.108, 48–54.
- [40] J de Prado et al., *Development of brazing process for W– EUROFER joints using Cu-based fillers*, *IOPscience, Royal Swedish Academy of Sciences Phys. Scr. T167* (2016) 014022.
- [41] J. de Prado, et al., *Improvements in W-EUROFER first wall brazed joint using alloyed powders fillers*, *Fusion Engineering and Design* (2017), Vol.124, 1082-1085.
- [42] L. Penga et al., *Microstructural and mechanical characterizations of W/CuCrZr and W/steel joints brazed with Cu-22TiH₂ filler*, *Journal of Materials Processing Technology* (2018), Vol. 254, 346–352.
- [43] W. Zhu et al., *A Ti-Fe-Sn thin film assembly for joining tungsten and reduced activation ferritic-martensitic steels*, *Materials and Design* (2017), Vol. 125, 55–61.
- [44] W. Krauss et al., *Performance of electro-plated and joined components for divertor application*, *Fusion Engineering and Design* (2013), Vol. 88, 1704–1708.
- [45] Q. Cai et al., *Diffusion brazing of tungsten and steel using Ti–Ni liquid phaseforming interlayer*, *Fusion Engineering and Design* (2015), Vol. 91, 67–72.
- [46] B.A. Kalin et al., *Development of brazing foils to join monocrystalline tungsten alloys with ODS-EUROFER steel*, *Journal of Nuclear Materials* (2007), Volumes 367–370, 1218–1222.

- [47] N. Oono et al., *Microstructures of brazed and solid-state diffusion bonded joints of tungsten with oxide dispersion strengthened steel*, *Journal of Nuclear Materials* (2011), Vol. 417, 253–256.
- [48] T. Chehtov et al., *Mechanical characterization and modeling of brazed EUROFER-tungsten-joints*, *Journal of Nuclear Materials* (2007), Volumes 367–370, 1228–1232.
- [49] Y. Ma et al., *Microstructure and Mechanical Properties of Brazed Tungsten/Steel Joint for Divertor Applications*, *Materials Science Forum* (2014), Vol 789, 384-390.
- [50] Z. Wang et al., *Investigation of Tungsten/steel Brazing using Nb Interlayer*, *Materials Science Forum* (2015), Vol. 817,27-34.
- [51] D. Bachurina et al., *Joining tungsten with steel for DEMO: Simultaneous brazing by Cu-Ti amorphous foils and heat treatment*, *Fusion Engineering and Design*.
- [52] D. Bachurina et al., *High-temperature brazing of tungsten with steel by Cu-based ribbon brazing alloys for DEMO*, *Fusion Engineering and Design* 146 (2019) 1343–1346.
- [53] D. Bachurina et al., *Joining of tungsten with low-activation ferritic–martensitic steel and vanadium alloys for demo reactor*, *Nuclear Materials and Energy* (2018), Vol. 15, 135–142.
- [54] D. Bachurina et al., *2020 IOP Conf. Ser.: Mater. Sci. Eng.* 1005 012010.
- [55] W. Liu, et al., *Investigation of tungsten/steel brazing using Ta and Cu interlayer*, *Fusion Engineering and Design* (2016), Vol. 113, 102-108.
- [56] J. de Prado, et al., *Effect of brazing temperature, filler thickness and post brazing heat treatment on the microstructure and mechanical properties of WEUROFER joints brazed with Cu interlayers*, *Journal of Nuclear Materials* (2020), Vol. 533, 152117.
- [57] J. de Prado, et al., *Thermomechanical characterisation of W-EUROFER 97 brazed joints*, *Journal of Nuclear Materials* (2020), Vol. 542, 152504.
- [58] V. Casalegno et al., *One-step brazing process for CFC monoblock joints and mechanical testing*, *Journal of Nuclear Materials* (2009), Vol. 393, 300–305.
- [59] J. de Prado et al., *Effect of Cr and V coatings on W base material in W-EUROFER brazed joints for fusion applications*, *Fusion Engineering and Design* (2020), Vol. 159, 111748.
- [60] C. Spadaro et al., *Laser surface treatments for adhesion improvement of aluminium alloys structural joints*, *Radiation Physics and Chemistry* (2007), Vol. 76, 1441–1446.
- [61] P. Šugár et al., *Laser surface texturing of tool steel: textured surfaces quality evaluation*, *Open Eng.* 2016.

[62] <https://www.sidermariotti.it/acciaio-inox/austenitici/316l.html>.

[63] A.Paùl et al., *Phase transformation and structural studies of EUROFER RAFM alloy*, *Materials Science Forum* (2006) Volumes 514-516, 500-504.